Summary

List of figures

List of tables

1. History of pollution and relative legislation

1.1. CO2 and its role in global warming

During the 18th century observations regarding giant boulders scattered mainly across Europe, far from the Alpine mountains, rose the obvious question of how they managed to get there.

The answer was not so obvious at the time. Although a French cartoonist 2 centuries later could have suggested that they were moved by a giant Gaul with the help of a special potion, at the time the main suggestions were Noah's flood and volcanic activity. The former was in fact the closest to the reality, as suggested by the mining engineer Jean de Charpentier, while observing giants blocks of granites in the Rhone Valley during the 1830s. It was in fact water (from the chemical point of view) what did transport these blocks, but in the form of ice. A Swiss-American renowned biologist named Louis Agassiz proposed at the Helvetic Society during 1837 that the Earth had been subject to a past Ice Age, proposing a comprehensive model that included an outflow of large glaciers from the Alps to the plains of Europe, Asia and North America, thus explaining observations made even by Goethe.

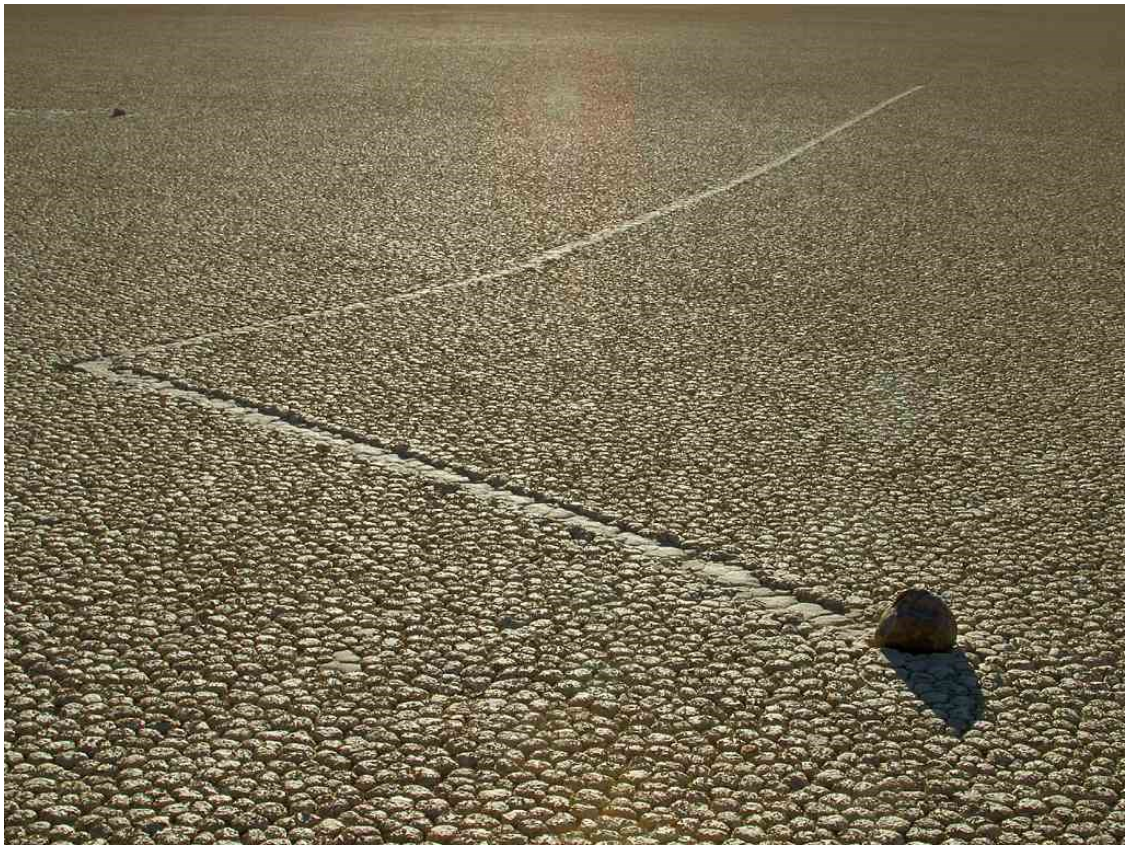

Figure 1 - Famous sailing rocks moved by thin sheets of ice in the Death Valley National Park, California

But while the effect of the ice age was clear and the scattering of giant boulders had a cause, the ice age itself was not explained by some cause of its own. It is not fully explained even now, but famous scientists aimed to answer the question. A partial answer is given by the astronomy regarding the deviations in earth orbits, defined as Milanković cycles. But the most interesting part is the radiative heat reflected by the atmosphere, or the so called "greenhouse" effect. The French mathematician and physicist Joseph Fourier developed the basic concepts of planetary energy budget and greenhouse effect, even though it never made the parallelism with the greenhouse. It noticed the fact that the atmosphere is opaque to "dark heat", also kwon as infrared radiation for the time, but he couldn't identify a root cause for this effect. An Irish physicist called John Tyndall some decade later discovered that infrared absorption is largely due to carbon monoxide and water vapor. He even proposed the correlation between CO2 and water vapor and the discoveries of the geologists, but a quantitative proof was needed.

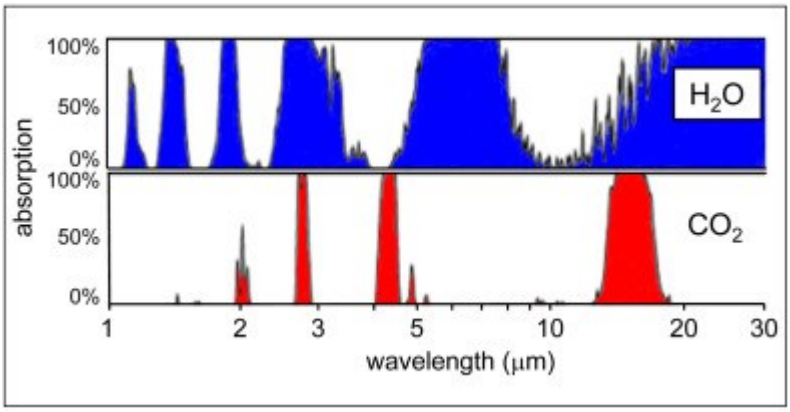

Figure 2 - Wavelength absorption of CO2

A Swede physicist, later a Nobel prize in Chemistry (1903) for his work on the conductivities of electrolytes, Svante Arrhenius. His interests in the field of chemistry, physics and mathematics led him to a mathematical analysis of the influence of CO2 on planetary energy budget in an article called "On the influence of carbonic acid [CO2] in the air upon the temperature of the ground." His study started from the measurements made by the American Physicist Langley using a bolometer (an instrument invented by himself) to parametrize absorption, dividing the earth surface in latitudinal sections of 10° and assigning a mean temperature for each one in each of the four seasons, while defining and assigning many other parameters, acceptable and consistent even today. His calculation took one year of his time and were set with different levels of concentrations of CO2 in the atmosphere, ranging from 0.67 to 3.0 the concentration measured at the time.

His results were that doubling or halving the CO2 in the atmosphere a variation of 5-6 degrees (respectively increasing or decreasing) could be expected. This was a result reassuring for him, since if the concentration didn't drop under the 0.62-0.55 of the time another ice age was distant, and the known production and increase of the CO2 due to industrialization was seen as a benefit for multiple reasons, one for all making warmer and thus more hospitable the lands of Sweden and Russia, even incurring in new cultivable lands.

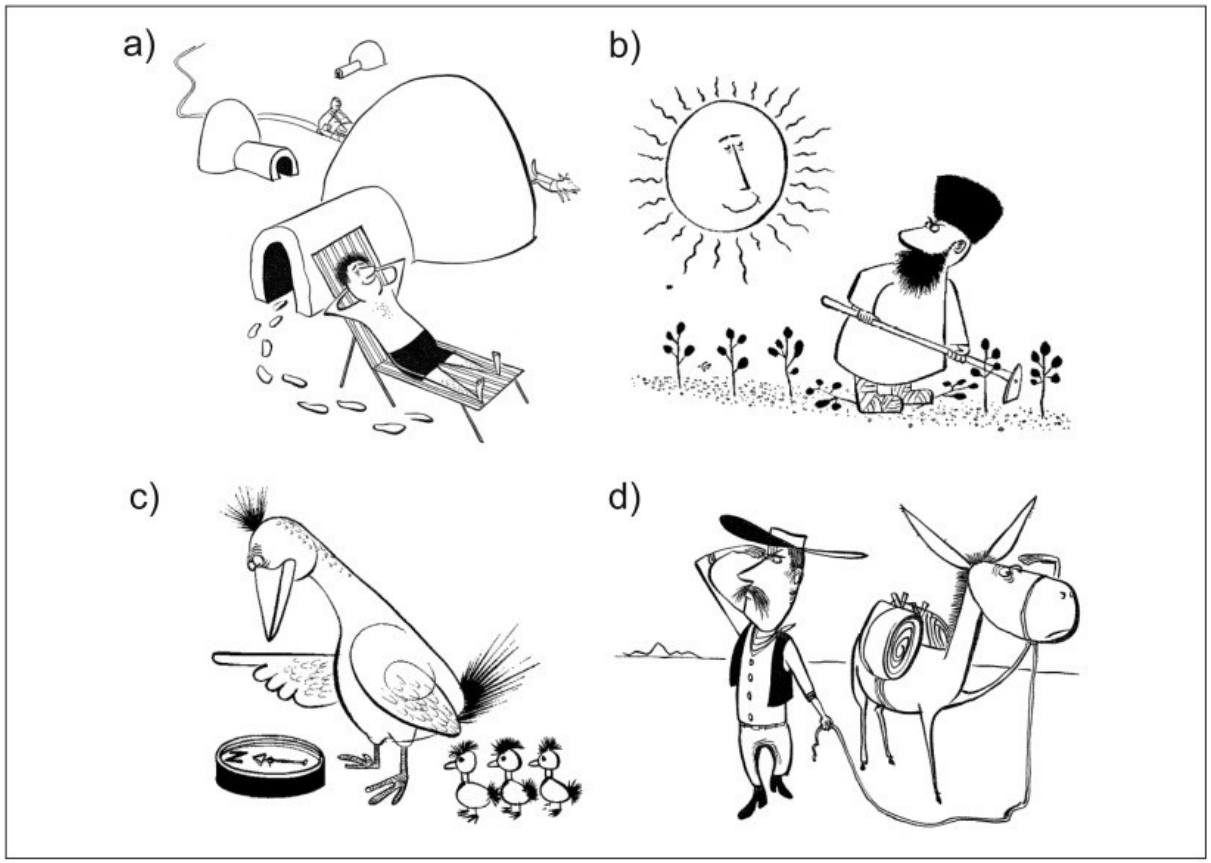

Figure 3 - Cartoons illustrating the ''benefits'' of warming climate: (a) the Arctic warms up; (b) nature at last smiles on the Russians; (c) northward migration of animals; (d) drought: water, water – but where?

A later study of an Englishman, Guy Stewart Callendar, during the 1930s tried to enhance the work of the swede Nobel prize, passing from a theoretical proof to an experimental one. With the help of a series of measurement called "World Weather Records" published yearly by the Smithsonian institute he analysed the temperature variation recorded from the 1880 until 1935 and correlated it with the measurement of CO2 concentrations made at the time, with some adjustments. His model enhanced the work of Arrhenius, taking in consideration the infrared absorption spectrum of CO2 developed by Rubens and Aschkinass and dividing the earth atmosphere in vertical sections regarding temperature, water

vapor and CO2 contents. As his predecessor, he used the water vapor as a feedback.

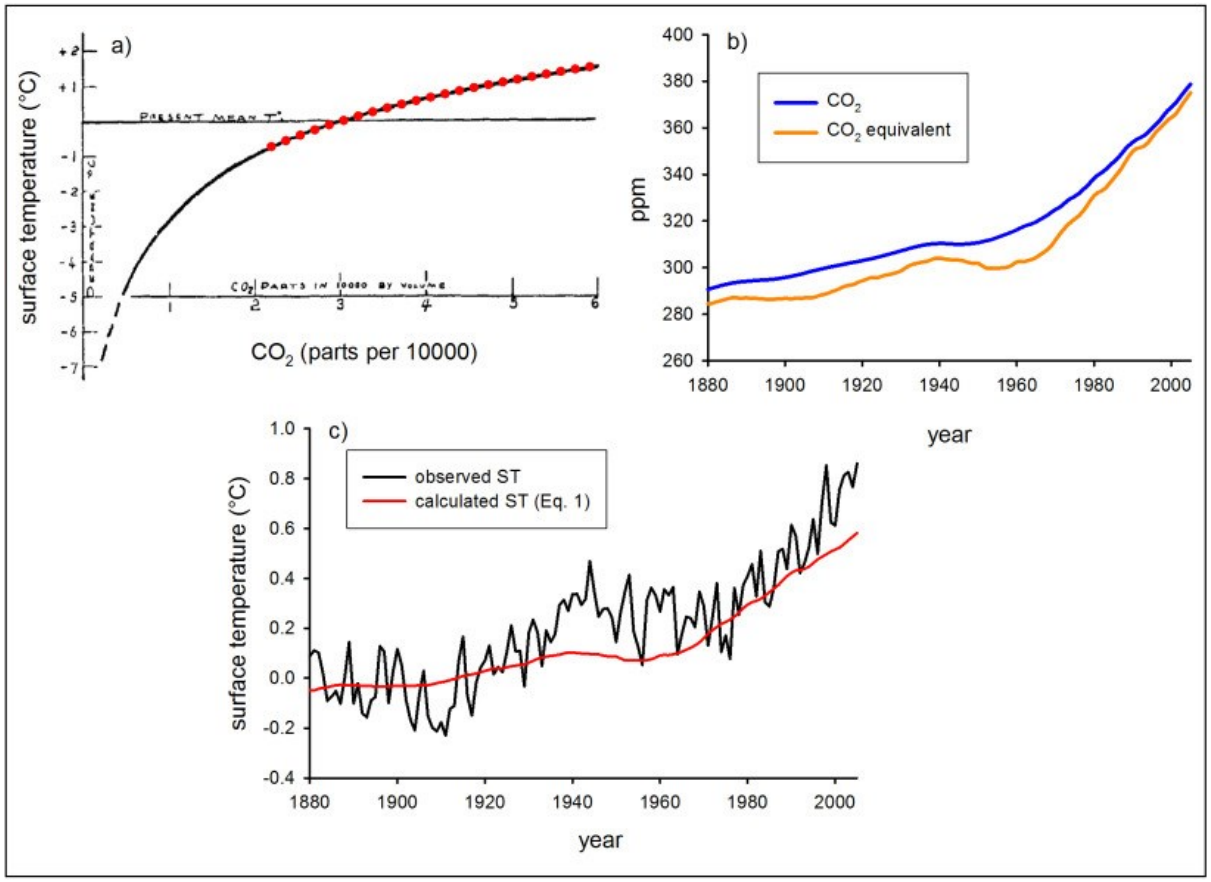

Figure 4 - Callendar correlation of CO2 and surface temperature

His calculation showed that at least 0.16° C of the 0.6 ° C temperature increase was caused by the CO2 concentration, but he incurred in two problems. The main was that the CO2 measurements were too much conservative, while he didn't consider effects caused by other greenhouse gases such as methane, NOx and chlorofluorocarbons, since these effects were completely unknown.

A large debate in the scientific community started concerning the buffer role of the oceans, that could store much of the produced CO2, up to fifty time the atmospheric one. The debate was resolved during the 1956 International Geophysical Year when the measurements of Keeling at the Manua Loca Volcano in Hawaii showed the yearly increase of CO2 concentration in the atmosphere, definitively proving the correlation between CO2 emissions and temperature increase.

According to Representative Concentration Pathways scenarios, without taking effective countermeasures in order to reduce CO2 emissions (switching to alternative non-fossils resources, improving efficiency by a large amount, limiting

land utilization for agricultural purposes and containing population growth) an increase in the global mean temperature by the 2100 is unavoidable, up to 4.8° C at the 95% confidence level of RCP 8.5, whereas scenarios with an aggressive reduction of CO2 emissions as RCP 2.6 could contain it in the range 0.3-1.7 ° C.

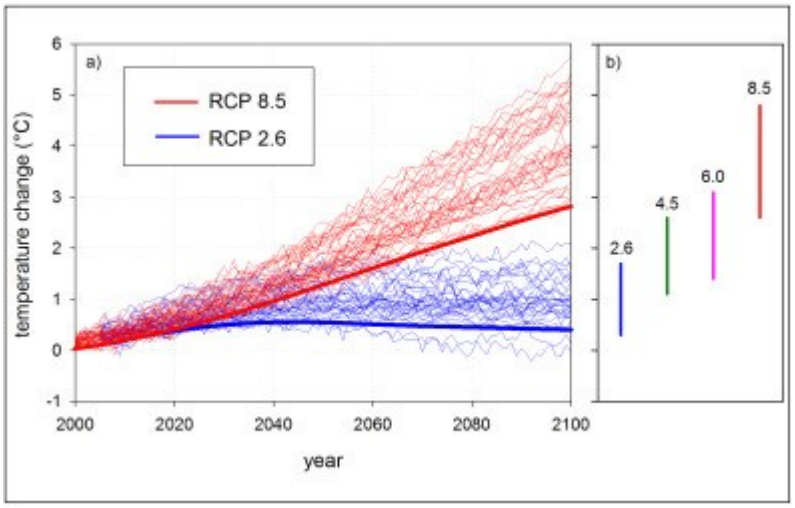

Figure 5 – Different Representative Concentration Pathways

The battle against global warming and air pollution is both local and global, even if sometimes it seems counterintuitive. For examples NOx and PN concentrations in urban areas resents greatly of the local meteorological conditions (due to temperature inversion phenomena and anti-cyclonic effects) which are due to the global climate change. The odd point is that for Diesel fuelled combustion engines the NOx and PM emissions could be lowered increasing fuel consumption and CO2 emissions, thus with the threat of nullifying or at least attenuating the benefits of the reduced NOx and PM emissions.

1.2. Transportation sector and pollution

The role of the transportation sector in CO2 and other greenhouse gases emissions has been investigated for years. The breakdown of GHG emissions by sources for the year 2010 is reported below, according to the IPCC.

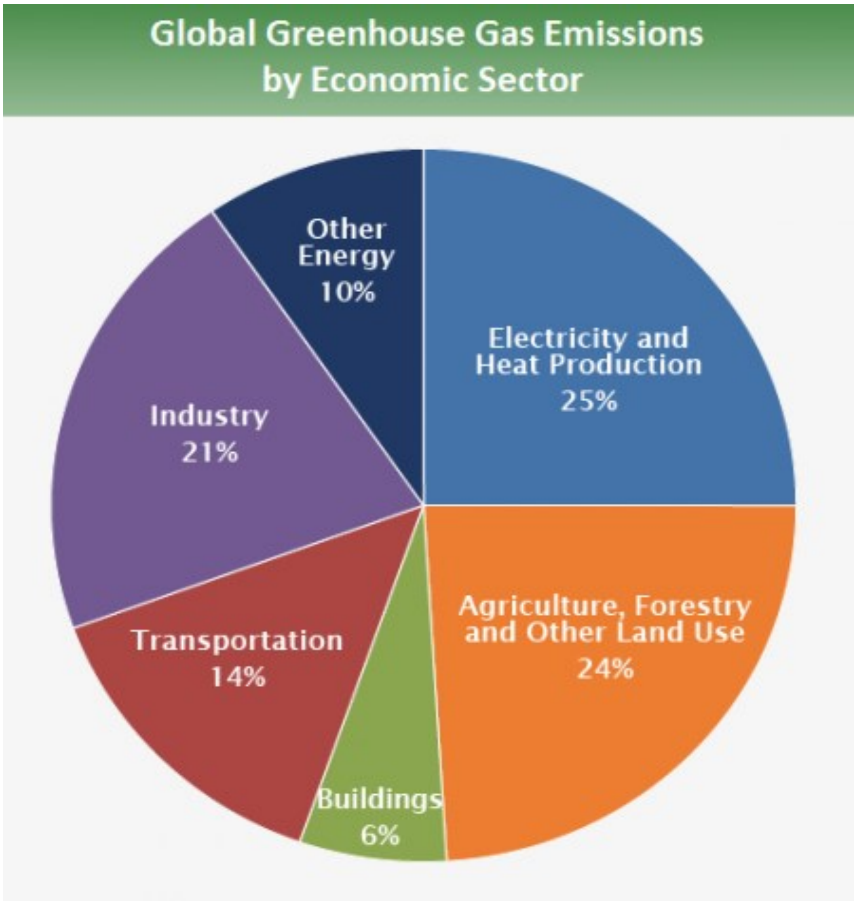

Figure 6 - Global GHG emissions by economic sector (IPCC 2010)

The emissions of GHG connected to the transportation rose by a 2.5 factor from the 1970 until today, increasing faster than any other energy end-use sector, bringing the CO2 emissions from 2.8 to 7.0 Gt of CO2 equivalent (other GHG gases account typically for about 5% in this sector).

The breakdown in the different modes available, especially when calculated over time, clearly shows that the principal contributor to GHG emissions is the road transport sector. While in the 40-year period taken into consideration the other modes together only nearly their absolute contributions, the road sector practically tripled its absolute contribution and rose about 20% in its relative contribution.

The road transportation sector alone contributes to about 10% of GHG worldwide emissions.

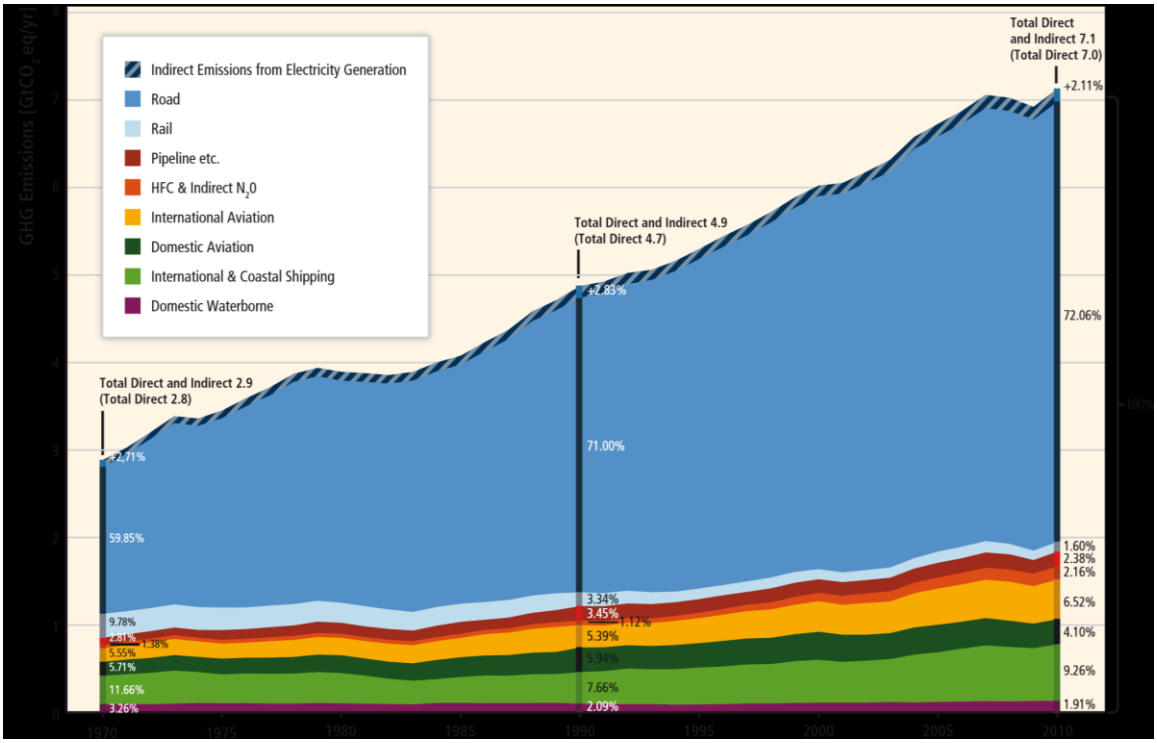

Figure 7 - GHG emissions breakdown for the Transportation sector

It could be noted that the relative contribution between 1990 and 2010 of the road sector remained practically constant with just a slight increase. The reason for the reduced increase in their relative contribution, despite the constant and nearly exponential growth in Light Duty Vehicles and Heavy-Duty Vehicles due to globalization and economic growth, is substantially the regulations applied by practically all the developed (and with less stringent regulations also underdeveloped or developing) countries to pollutant emissions to the road transportation sector.

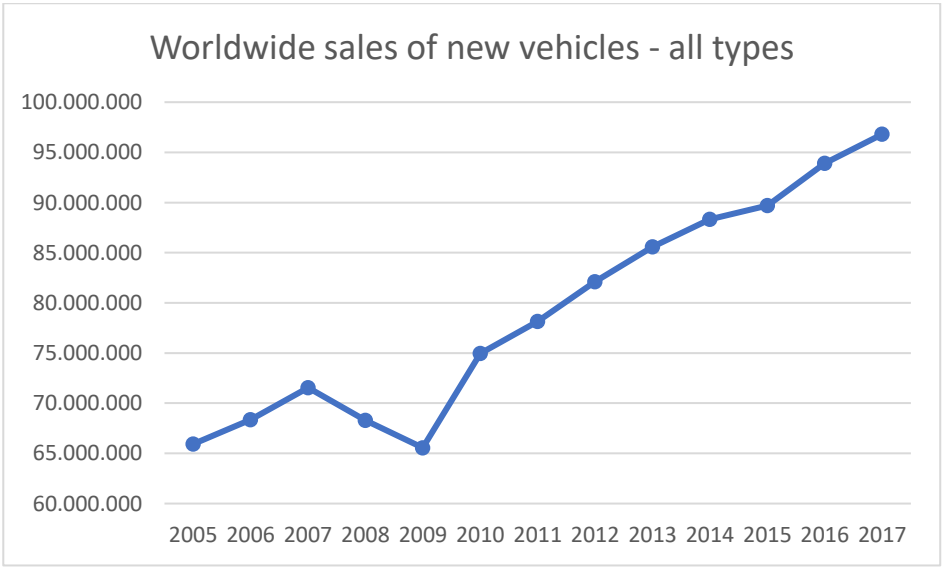

Figure 8 - Worldwide sales of new vehicles (OICA, March 2018)

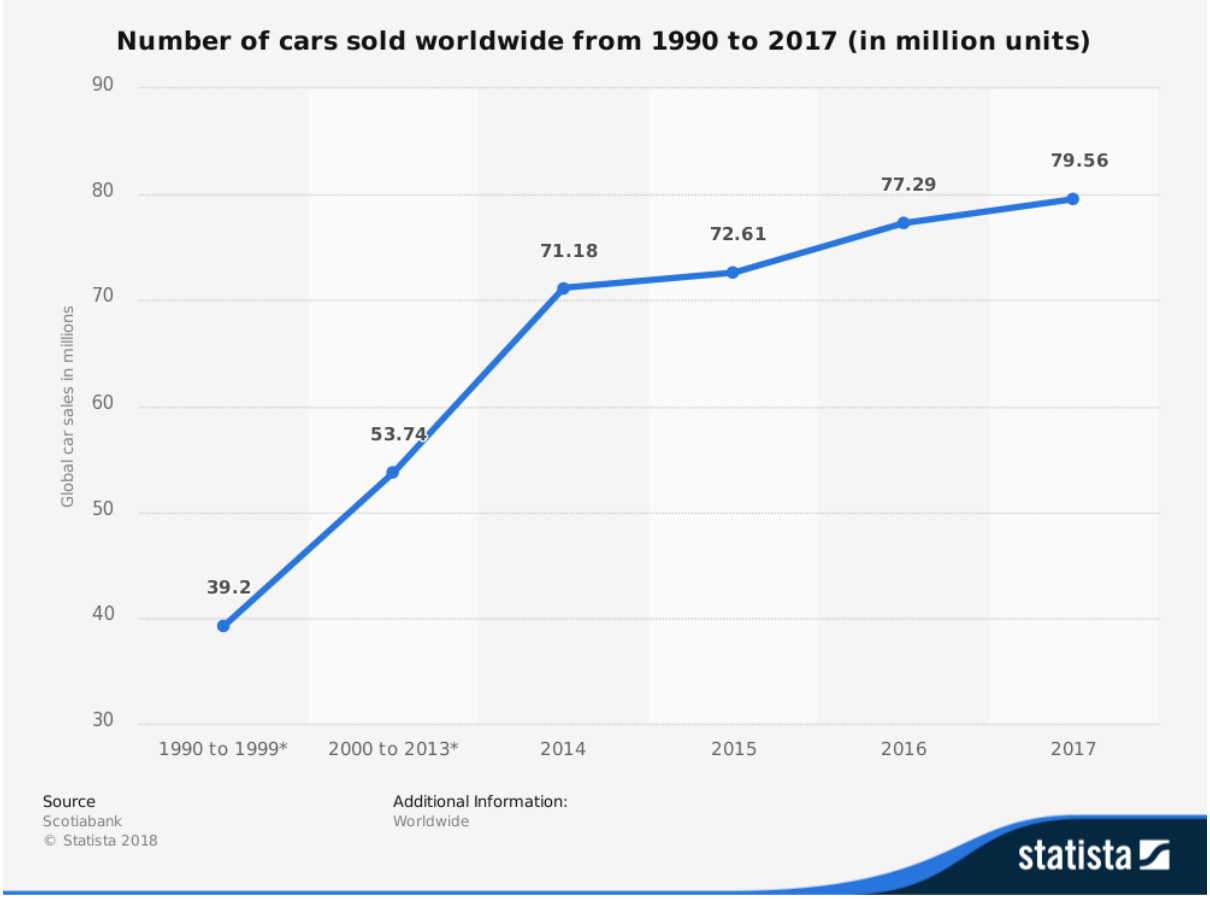

Figure 9 -Worldwide sales of cars (Statista)

From the graphs above we can notice that the sales of new vehicles are constantly growing due to the opening of new markets as China and India and to the broadening of the economic power of lower and middle classes in other countries such as Eastern Europe, Turkey, South Africa, Southern and Central America.

Only regulations could counterbalance this rapid growth in vehicles presence worldwide, since from the actual 1.2 Billion Vehicles on the road we will reach the 2 Billion by 2035.

1.3. Pollution disasters and early pollution legislation

Regulations began to appear in the automotive industry in the 1950s in California. Due to the mass motorization of the post-war period and the intensive activity of industries some cities, in conjunction with exceptional climate events, began to suffer pollution crises, even with the event of deaths.

A temperature inversion (the air above the surface hotter than the air at the surface level) led to a 5-day crisis in the steel mill city of Donora, Pennsylvania, during 1948. During the last day of the sulphur dioxide and hydrogen fluoride pollution crisis upon the 30th of October, 17 peoples died because of respiratory

complications, and 4 more died the day after for the same reasons. 43% of the residents fell ill, and even a decade after the death ratios were higher than nearby cities. Only the halt of the production and a consequent rain on the day of the Sunday 31st of October took the situation in containment. The zinc factory was considered the biggest culprit, since for hundred meters the vegetation around there totally disappeared due to the fluorine gas emissions.

Figure 10 - Donora disaster

Another known episode occurred in the city of London from the 5th to the 9th of December 1952, due to an anticyclonic windless condition in conjunction with the cold weather that pushed the Londoners to increase their coal consumption. The exceptional events killed at least 4,953 people according to medical records of the days but estimates of February brought the death toll to 6,000 persons and 25,000 obtained sickness benefits, mainly elderly and children. Later estimates further increase the death number to 12,000. The smog (the contraction of smoke and fog, a word coined by a Londoner doctor in 1905 to describe the thick layer of smoke that resembled fog) was so critical that was suspended every public transport (apart from the underground) and even the ambulance social service, since it was impossible to drive with a visibility reduced to few meters. It penetrated even inside closed space, resulting into cancellation of concerts and film projections. The Prime Minister Winston Churchill defined the crisis as a “meteorological accident”, but later legislation began to take countermeasure to reduce emissions due to coal usage in households, both for cooking and for heating purposes.

Figure 11 -Trafalgar square during the Great Smog, 1952 London

Part of the cause of the 1952 Great Smog was due to diesel-fuelled buses that replaced the electric trams between October 1950 and July 1952, due to post-war economic problems with electricity availability (aggravated by the increase in average price of electricity subsequent to the 1948 nationalization of producers) and steel shortage for maintenance as well as "aesthetic reasons" concerning wires and noise and supposed improvements in traffic flows.

Another interesting episode occurred during WW II in the city of Los Angeles. During the 26th of July 1943 a dense smog cloud surrounded the city, resulting in a public fear of a Japanese chemical warfare. Because of wartime migrations and infrastructure planning L.A. became the largest car market of the U.S. Industries and the presence of two large ports in the area contributed to the sudden rise in emissions favoured by particular geographical and microclimatic conditions. In fact

Los Angeles is located near a basin of the Pacific Ocean, is surrounded by close mountains that prevent air circulation away from the ocean, and because of these two geographic conditions has lots of sunny days and low rainfall. The sunny days contributes to photochemical smog formation, while the low rainfall tends to leave the aerosols suspended in the air. In 1943 the culprit was identified as a factory that used a new process for manufacturing synthetic rubber. But the quick shutdown of the factory (the Angelenos were very proud of their air "that could cure tuberculosis and alcoholism") didn't manage to significantly improve the quality of the air.

Figure 12 - Los Angeles air pollution during 40's

In 1947 the use of coal was banned in the entire area and some investigations began, since the stinging and air lung irritation became too significant to be ignored. One of the member of the "Dutch Mafia" at Caltech, Arie Jan Haagen-Smit began to investigate the cause of these damages, that led even to crops damage and rubber cracking. Observing the rubber cracking during the hours of the day he managed to measure the ozone concentration and connected his studies of

photosynthesis to the formation of Ozone layers, effectively discovering the process of creation of photochemical smog.

The work of Haagen-Smit at Caltech published during 1952 was contested during a lecture at the university by another chemist of the Stanford Research Institute, organized by Beckman, another researcher of the passenger vehicle pollution in the L.A. area. The plot of Beckman was to make Haagen-Smit's pride wounded in such a way that the Dutch would double his effort towards finding the causes of the smog that had such severe effects on the health and on the economy of the Californians.

The studies and the advocacy for improvement in air quality, once the scientific circles accepted the studies of Haagen-Smit and Beckman by mid 1950s, led to scientific movements and citizen movements that began to pressure the politician to pass legislation to reduce pollution, since the carmakers were reluctant. In 1953 an inquiry of the Los Angeles County Supervisor to the Detroit carmakers whether they were studying the effects of tailpipe emissions received a vague answer, so in 1961 the California state enforced a mandatory regulation regarding all new cars sold starting from 1963 equipping them with crankcase ventilation devices that alone contributed to 25% of hydrocarbons emissions. These efforts continued first with the creation of the California Air Resource Board in 1967 by the governor Ronald Reagan and the appointment of both Beckman and Haagen-Smit in the CARB. Three years later, during 1970, the president of the United States Richard Nixon signed the Clean Air Act, forming the EPA and mandating a 90% reduction of emissions by 1975. These results were not enforced at the time, but the act posed the basis for the 1975 Energy Policy Conservation Act that defined fleet average fuel consumption standards, with the purpose of improving efficiency and reducing national fuel consumptions. These regulations were enforced starting from 1978 and are defined as CAFE standards and have a mechanism of penalties and temporary bonuses.

1.4. Early cycles and standards

But in order to enforce a standard it was necessary to implement a reference cycle, operated on the dynamometer. The test cycle chosen by EPA was a slight variation of the FTP-72 cycle (Federal Teste Procedure 1972) called FTP-75. In figure 13 is reported the cycle trace.

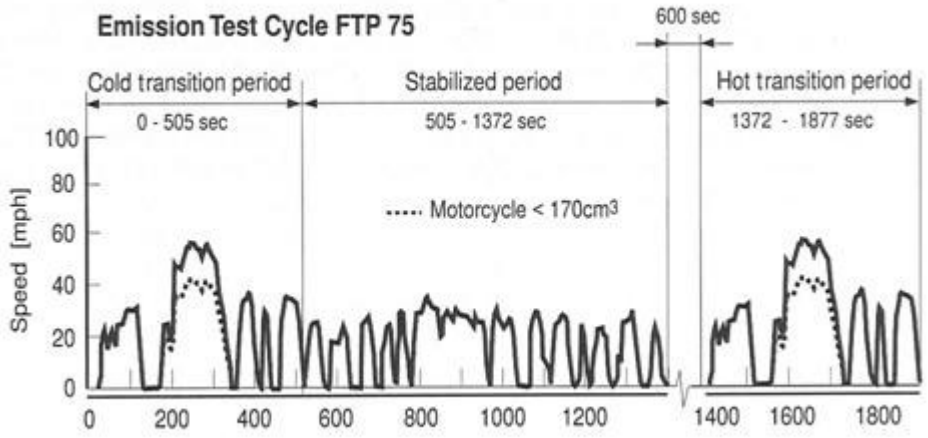

Figure 13 - FTP 75 Cycle

In Europe at the same time various countries adhered to the United Nation Economic Commission for Europe that began to regulate and standardize automotive homologations, to favour economic exchanges between different countries. The ECE produced various regulation, concerning lightning, electromagnetic compatibility, safety regulations, and environmental ones. Between them defined the ECE R 15 cycle, also known as Urban Driving Cycle.

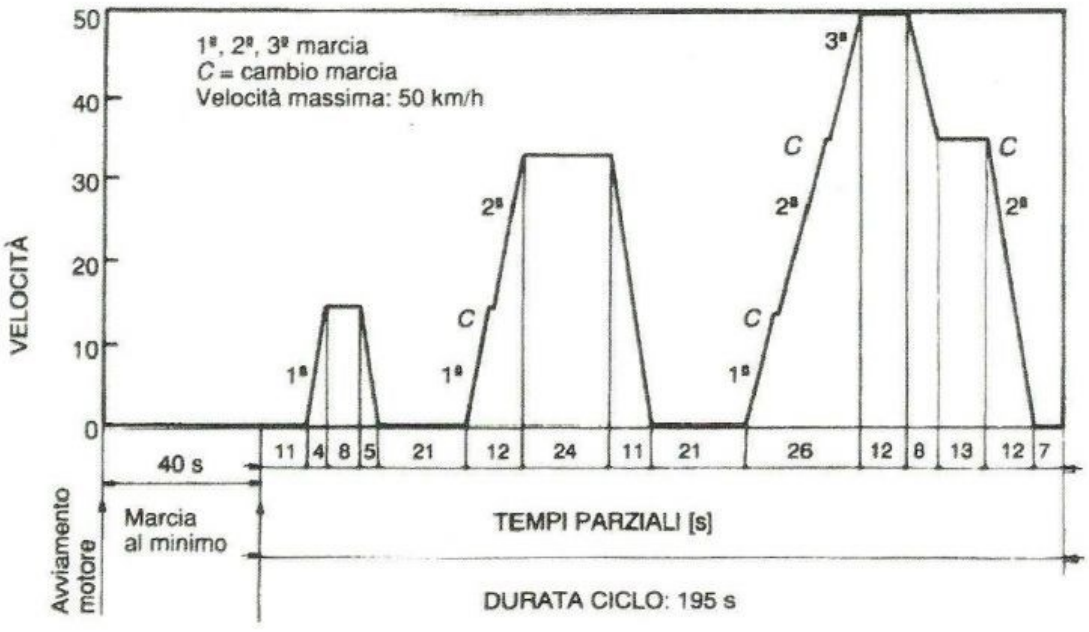

Figure 14 - ECE R-15 Cycle

It was repeated twice to find the fuel consumption of the type approved vehicles, then it was added the EUDC and the combination of the two formed the NEDC.

As it could be seen the ECE R-15 Cycle (and the EUDC) are not so demanding in terms of velocity and accelerations, their variability is low when compared to the

FTP-75 (later accompanied by another test cycle), thus impelling the severity of the cycle with respect to polluting agents. This is also partially due to test masses.

Europe also introduced Corporate Limit standards, but in the form of CO2 emissions, in order to tackle directly the CO2 emissions problem, while CAFE standards were more about fuel consumption and energetic dependency from foreign countries. In 2008 it was mandatory to reach a fleet average of 140 g/km (a reduction of 25% over 1995 levels) and a further target of 120 g/km was imposed for 2012.

Both CAFE standards and EU CO2 standards encountered the adversities of carmakers, bringing curious and creative solutions. One of the strangest was the creation of the Aston Martin Cygnet, practically a badge engineered Toyota IQ (the car with the lowest CO2 emissions in g/km at the time) in order to reduce the fleet average of the supercar carmaker, to not pay the penalties automatically issued for being above the standards for each vehicle. A rapid change in regulation neutralized this approach, since the fleet averages were not calculated on the number of car offered to the market but on the proportion of car sold. The Cygnet, given its enormous price tag (more than double the IQ for a series of luxury items such as handcrafted leather seats, handmade mechanical clock and other distinctive features of the Aston Martin brand), did sell very poorly and the last production batch was actually sold as an homage to the purchase of costly supercars.

In the US market, by admission of the famous CEO of Chrysler during ‘80s Lee Iacocca, Minivans and SUV (and even the Chrysler PT Cruiser) were created as passenger cars but respected the less stringent requirements of light trucks, encountering both an industry needs and creating in fact new markets segments that thanks to the marketing pushed the sales of this vehicles. Oddly, one of the heaviest and gas guzzling SUV, the Hummer H1, since it exceeded the maximum weight specified by the regulation, was not subject to the CAFE standards during its production.

It is evident that the more precise EU CO2 approach, with progressive penalties but also the possibility of having bonuses and the possibility to exchanging (thus selling) them between carmakers, is much more effective than the US approach but on the contrary, the US test cycles are much more effective in being close to the reality with respect to EU ones.

In 2009, since the 120 g/km could be not attained effectively by 2012, the European Commission defined a limit value curve for test mass. The emissions between 2017 and 2020 were lowered to fleet standards of 95 g/km, with a further 25% reduction.

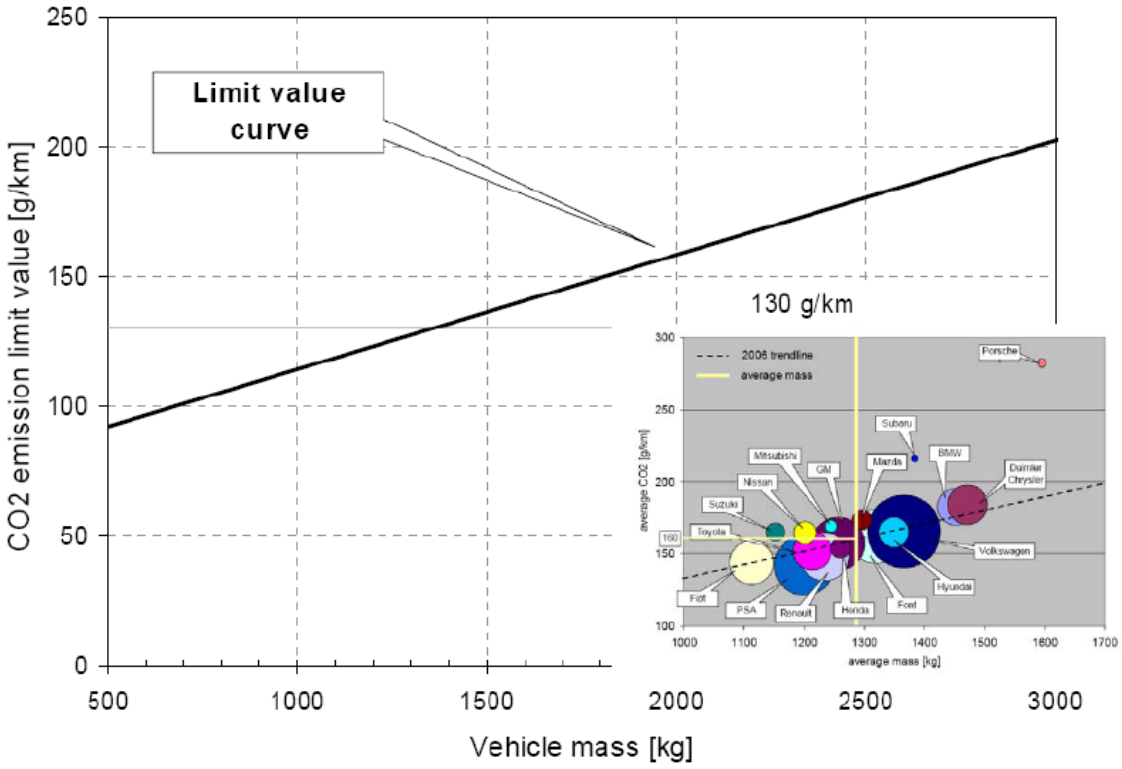

Figure 15 - 130 g/km limit curve

But there are some deficiencies in the NEDC cycle and its test procedure. The NEDC is composed by 4 repeated ECE-15 cycles and then a EUDC Cycle. Its maximum velocity is 120 km/h with defined gears and gentle and constant acceleration by today standards. It must be added that the test mass is not fully representative of the actual mass of the vehicle (accessories could be excluded according to the legislation and only the additional weight of the driver is accounted for) and also the measurement of road-load coefficients is lower than the real one. Furthermore, the NEDC cycle doesn't consider road incline and harsh environmental conditions such as very cold start.

This results in big discrepancies between cycle and real driving emissions, so that the 85% reduction in NOx emissions limits between Euro 3 and Euro 6 (from 500 mg/km to 80 mg/km) achieved a mere 40% reduction of the real NOx emissions measured over the same time period (figure 16).

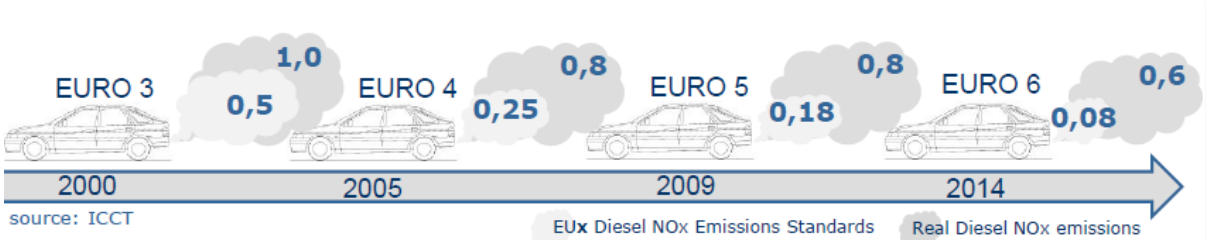

Figure 16 - Evolution of EU NOx Emission standards

The solution to reduce the discrepancies between real ones and driving cycles are essentially two: designing better driving cycle and better test procedures or abandoning the approach of driving cycles and through statistical data analysis and thanks to Portable Emissions Measurement Systems (PEMS) analyse real emissions during real driving conditions. The problem of this approach is that the test equipment is costly, it adds a considerable mass to the vehicle, is much costlier to achieve acceptable data (since more cycles are needed due to the variability of the environmental conditions) and due to the uncertainties of data it is harder to write a standard. Nonetheless these obstacles could be overcome, but for the moment the strategy is to pose Conformity Factors between RDE achieved through road testing and dynamometers cycle-based results, and to reduce the gap between them progressively. Namely the CF for NOx emissions according to EU regulation are 2.1 from 09/2017 (for new vehicles with a 2 years grace period for vehicles already on the market) until 01/2020 when it will be lowered to 1.5 (with again a one-year grace period for already homologated vehicles). Regarding CO2 the EC strategy is to phase-in the WLTP standard along the NEDC one, with the goal to acquire data useful to set subsequent more stringent standards. From 09/2017 it is mandatory the double testing for the new type-approved vehicles and by 09/2018 will be mandatory for every sold vehicle.

Emission Limits	Euro 5b			Euro 6b		Euro 6c				Euro 6d			
	2012	2013	2014	2015	2016	2017	2018	2019	2020	2021	2022	2023	2024
CO_2 Fleet	130 g/km					95 g/km - NEDC Based Target				To be Defined on WLTP test results			
Driving Cycle	NEDC Testing Only					Double testing NEDC/WLTP				WLTP Testing Only			
Low Temperature Test (-7°C) for CI Vehicles						Introduction				New Limits			
Real Driving Emissions						Phase-In				New Limits			

Figure 17 - Road map for current and future EU regulations

The work of the UNECE group during the last years had been to revise both the cycle and the test procedure, but at the same time making it Worldwide, in order to set a standard for a wider set of countries (the goal was to make it viable worldwide), thus facilitating the carmakers effort in producing and homologating new powertrains and favouring economic exchanges. The WLTP maintains a certain degree of "customization", since the test procedure is standardized, but the 4 different cycle phases (low, medium, high and extra-high) could be selected by each country through its legislation. For example, in India, due to traffic issues, lack of big highways and poor road condition the proposal is to set a cycle excluding the extra-high part but integrating with another phase, e.g. L+2M+H or 2L+M+H. In Japan the Extra-High phase is excluded due to their driving habits. Also, other results could be "tweaked" by local legislations, as for the case of the emission standards of the hybrid and electric vehicles.

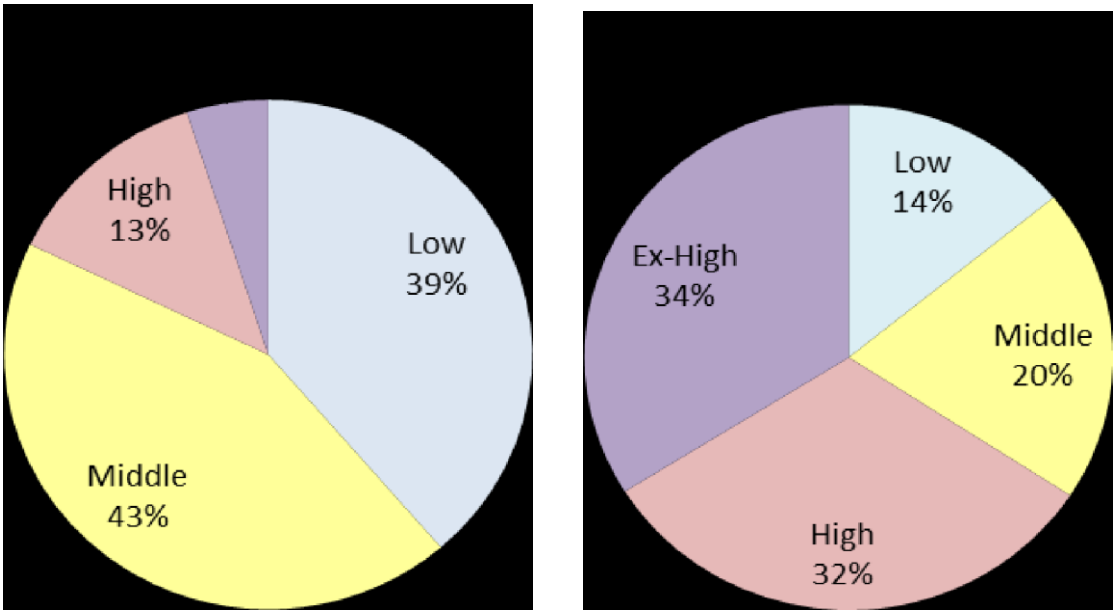

Figure 18 - Japan and Worldwide use profile

2. Changes in legislation and solution proposed by carmakers

2.1. NEDC and WLTP comparison through simulation of 2 known vehicles

NEDC and WLTP define the test mass according to the equations below.

$$TM_{NEDC} = UM + 100$$

$$TM_{WLTP} = UM + OM + 100 + 0.15 \cdot (LM - UM - OM - 100)$$

Where UM is the curb mass of the vehicle, OM is the mass of optional equipment and LM is the technically permissible laden mass.

The parameter for two different vehicles following NEDC and WLTP standard are reported in table 1.

NEDC - Vehicle 1				**NEDC - Vehicle 2**				
m	F0	F1	F2	m	F0	F1	F2	
1168	124,7	0	0,0364	1063	114,2	0	0,0344	
kg	N	N/(km/h)	N/(km/h)^2	kg	N	N/(km/h)	N/(km/h)^2	
WLTP - Vehicle 1				**WLTP - Vehicle 2**				
m	F0	F1	F2	m	F0	F1	F2	
1360	186	0	0,0419	1210	166	0	0,039	
kg	N	N/(km/h)	N/(km/h)^2	kg	N	N/(km/h)	N/(km/h)^2	
R				R				
289,3437				285,3648				
mm				mm				

Table 1 - NEDC and WLTP characteristics of 2 known test vehicles

The two vehicles, equipped with the same 1.3 Direct Injection Turbodiesel engine and the same gearbox with the characteristics reported in the table 2 and the fuel consumption and NOx emissions plotted in the figures 19 and 20.

J_eng	J_w	i_bsfc	i_n	fd	V
0,183	2,7794	315	800	835	1,248
kg*m^2	kg*m^2	g/h	rpm	g/l	dm^3
tau_1	tau_2	tau_3	tau_4	tau_5	tau_f
3,909	2,238	1,444	1,029	0,767	3,563
eta_1	eta_2	eta_3	eta_4	eta_5	eta_f
0,94	0,94	0,94	0,94	0,94	1

Table 2 - Powertrain characteristics of the vehicles

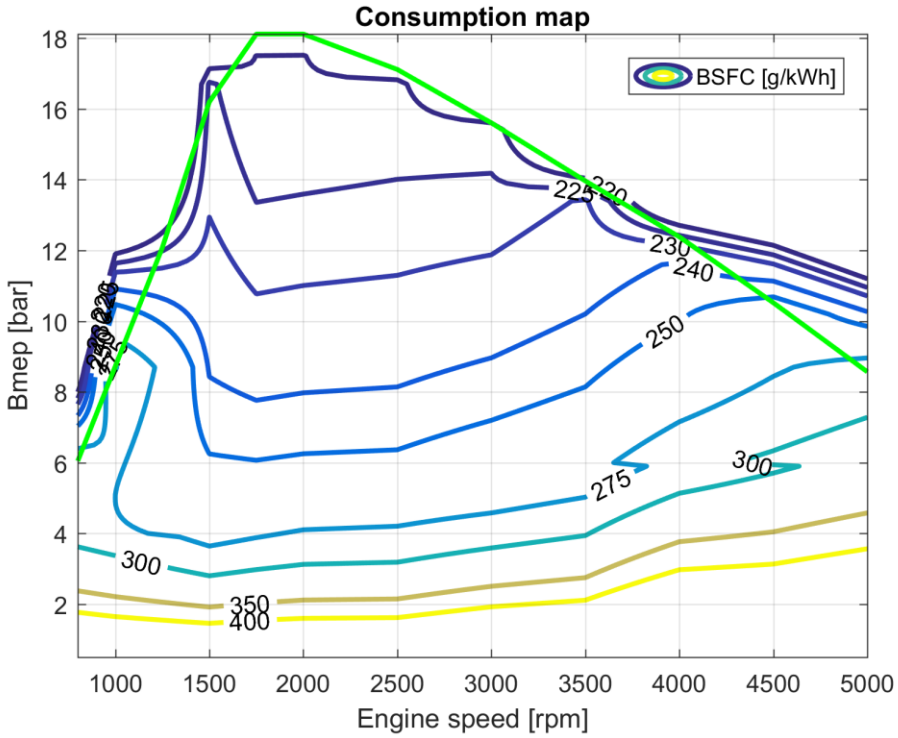

Figure 19 - Consumption map of 1.3 Turbodiesel CR II engine

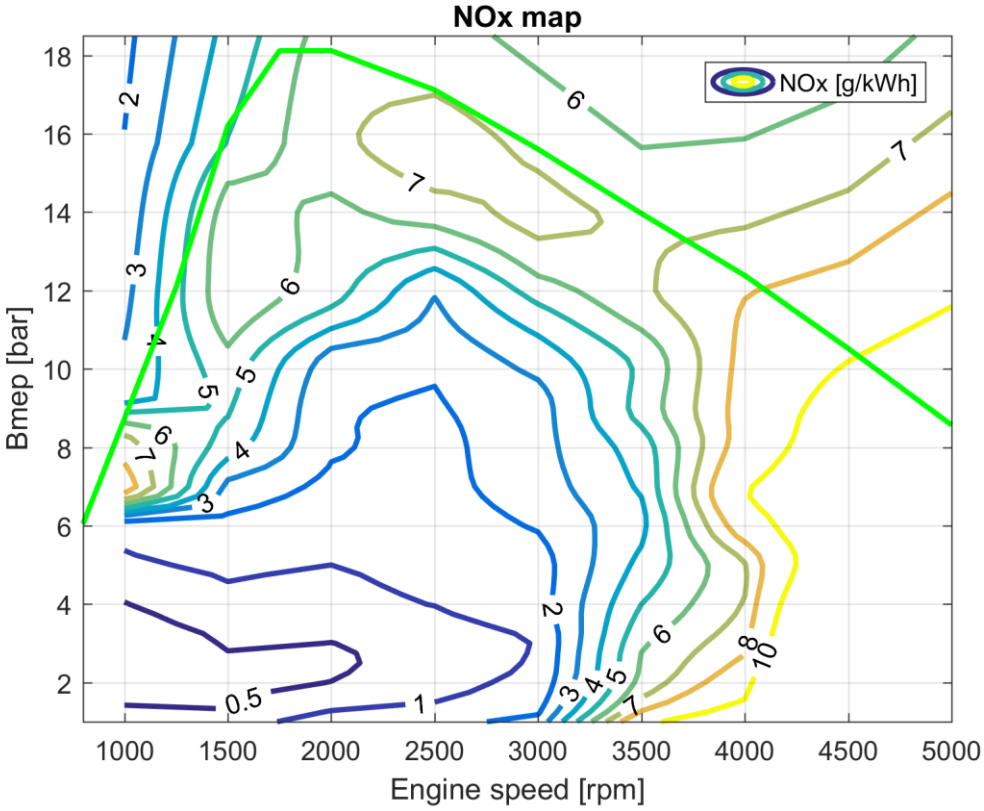

Figure 20 - NOx map of 1.3 Turbodiesel CR II engine

The two different cycle trace are reported in figure 21 and 22 respectively for NEDC and WLTP

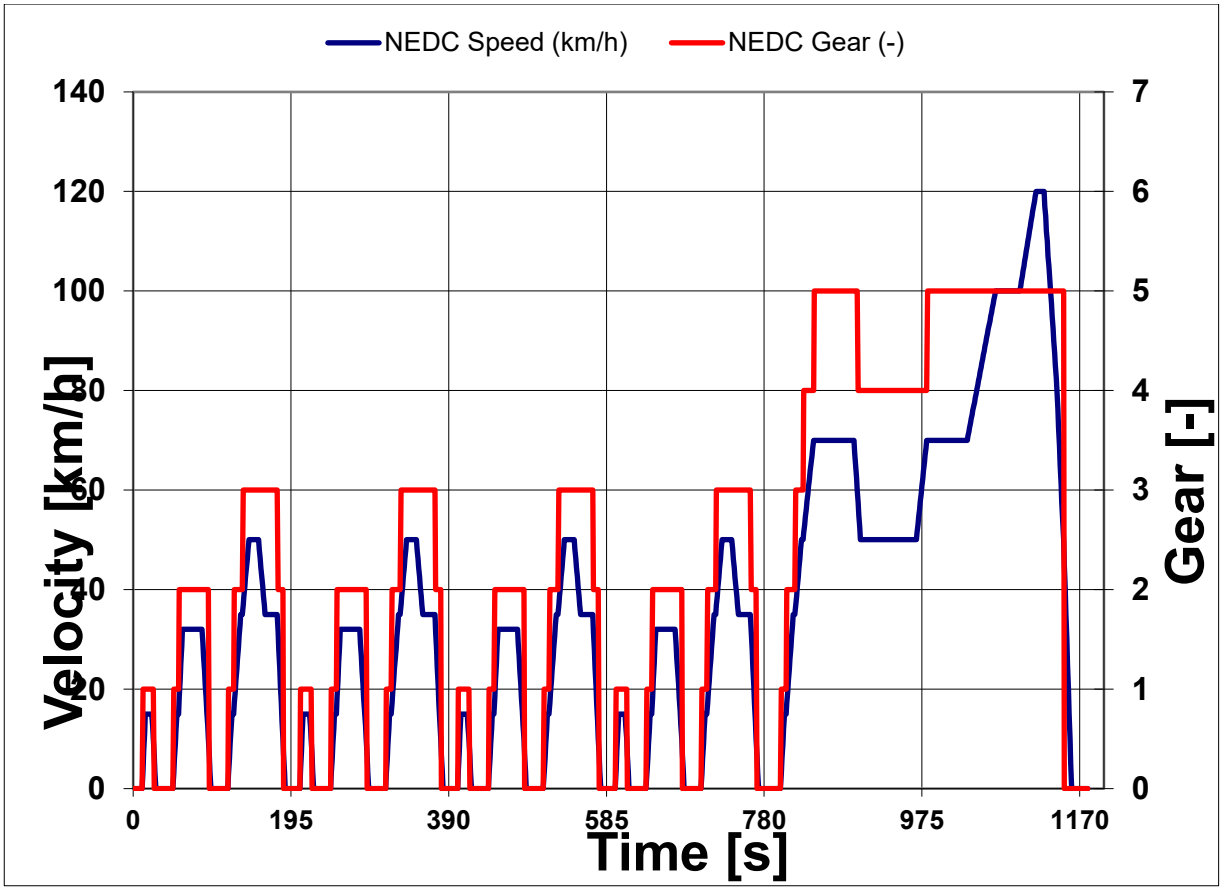

Figure 21 - NEDC cycle trace and gear changing strategy

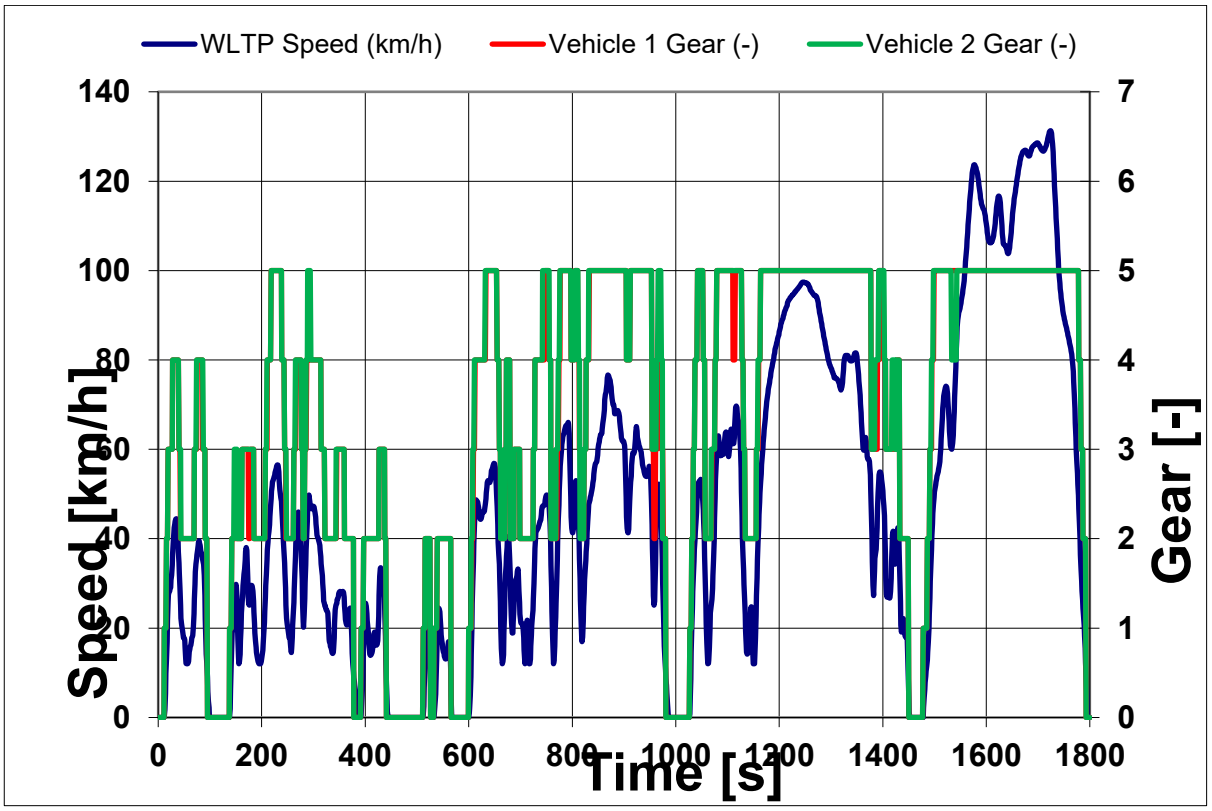

Figure 22 - WLTP cycle trace and gear changing strategy

Results for the two different test cycle and both vehicles are reported in figure 23 and 24.

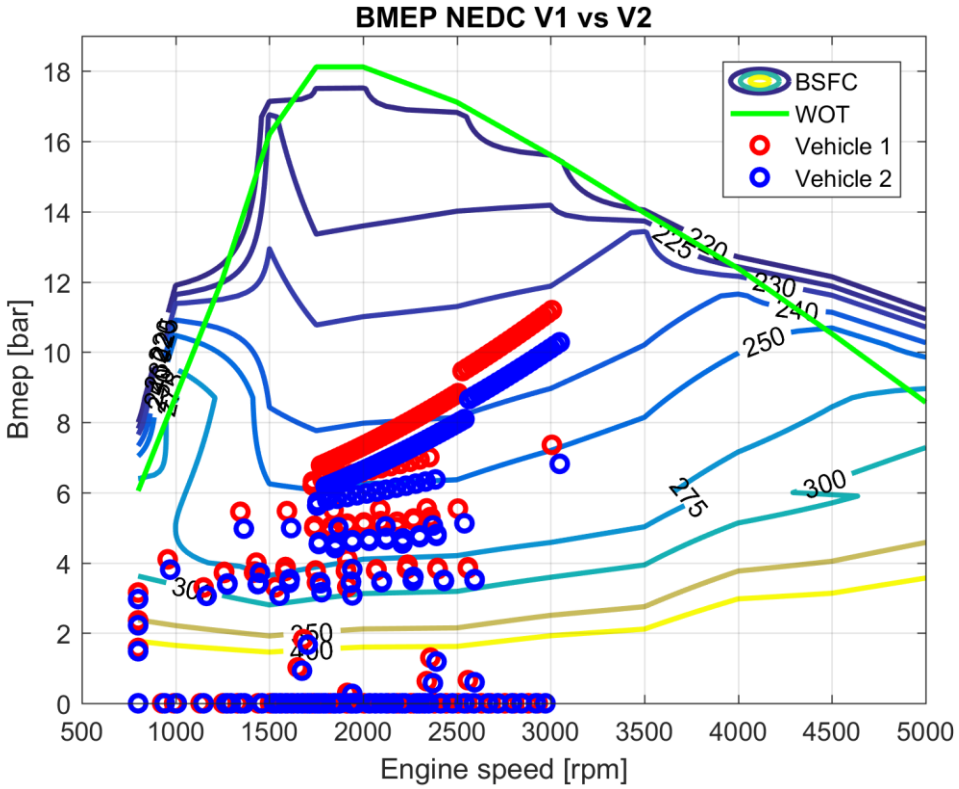

Figure 23 - BMEP for the two vehicles under NEDC

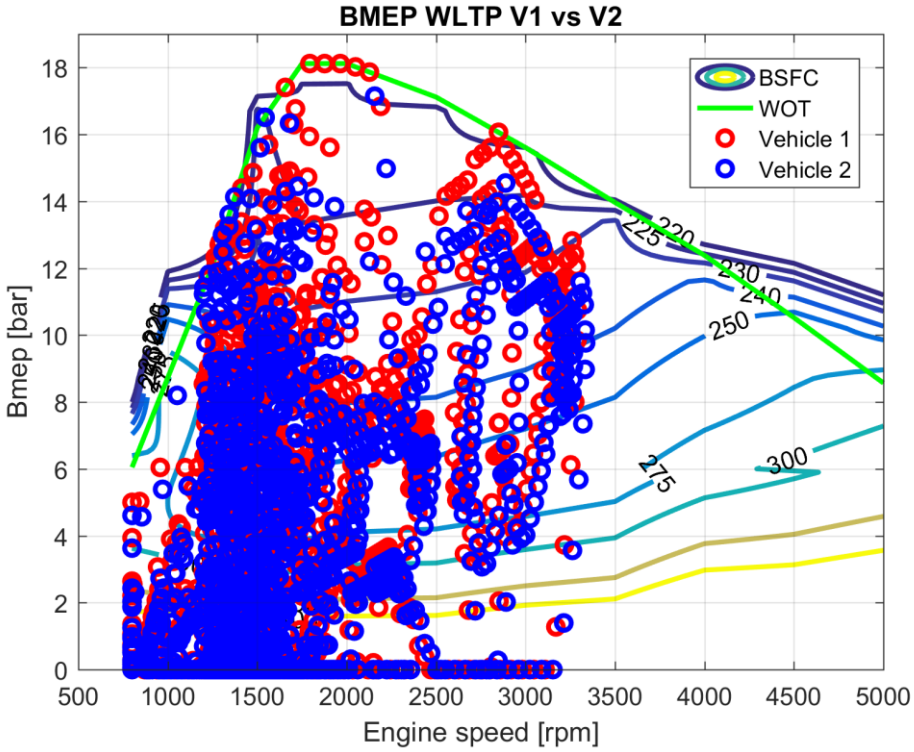

Figure 24 - - BMEP for the two vehicles under WLTP

Emissions and consumption, calculated by interpolation by the fuel consumption and NOx map through a proper simulation, are resumed in the table 3 for the two cycles and both vehicles. CO2 is calculated simply from the fuel consumption.

NEDC Vehicle 1			**NEDC Vehicle 2**		
Consumption	NOx	CO2	Consumption	NOx	CO2
4,662	0,184	123,59	4,482	0,156	118,82
l/100km	g/km	g/km	l/100km	g/km	g/km
WLTP Vehicle 1			**WLTP Vehicle 2**		
Consumption	NOx	CO2	Consumption	NOx	CO2
5,469	0,642	144,98	5,101	0,523	135,23
l/100km	g/km	g/km	l/100km	g/km	g/km
+17%	**+248%**	**+17%**	**+13%**	**+234%**	**+13%**

Table 3 - Emissions and consumption results for both vehicles under NEDC and WLTP

The WLTP is much more demanding in terms of BMEP (and torque) and this reflect heavily on the increase of NOx emissions (more than 3 times the emissions in terms of g/km), while the increase upon the fuel consumption is limited below 20%.

2.2. Current trends in the automotive industry to comply with regulations

Carmakers are taking different approach to comply with CO2 and NOx standards. First, it must be noted that the current and future legislation, especially in Europe is pointing toward a fuel neutral approach (more than ever the ones regarding PN and NOx), while until Euro 4 the limits were heavily differentiated. Contemporarily SI an CI are becoming much more similar, with both technologies utilizing Direct Injection, Variable Valve Timing Turbocharging, EGR (although for different purposes) ad Particulate Filters.

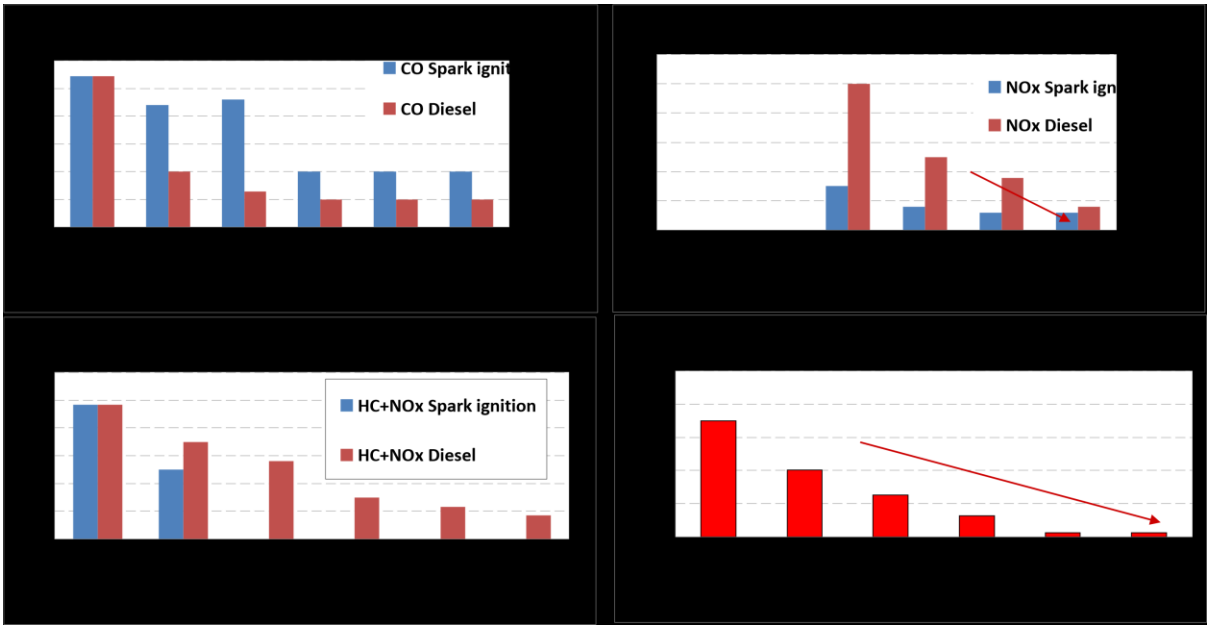

Figure 25 - Evolution of pollution limits in EU Regulations

Manufacturers are taking different paths to achieve the CO2 reduction. Practically all of them in the Gasoline field are switching to variable valve timing undersized turbo-charged directly injected engines. Variable Valve Timing was a major breakthrough during 80's and 90's and 2000s studies has taken this technology to achieve "full valve control" (controlling also the lift and duration of valve cycles) or Variable Valve Actuation during each operating condition of the ICE. The old MPI engines doesn't allow a full control of the mixture ignition, provided by the DI ones, and reducing the displacement and even the number of cylinders the friction losses are heavily reduced, while the power reduction is compensated by the injection pressure increase and the BMEP increase due to turbocharging Thanks to DI, VVA and turbocharging is possible to take advantage of scavenging, not attainable without these 3 enabling technologies. Even utilizing some "exotic cycles" (Miller Cycles, Atkinson) for certain engine operating conditions is much more common and is becoming recurring the application of cylinder deactivation, enabled once again by DI and VVA.

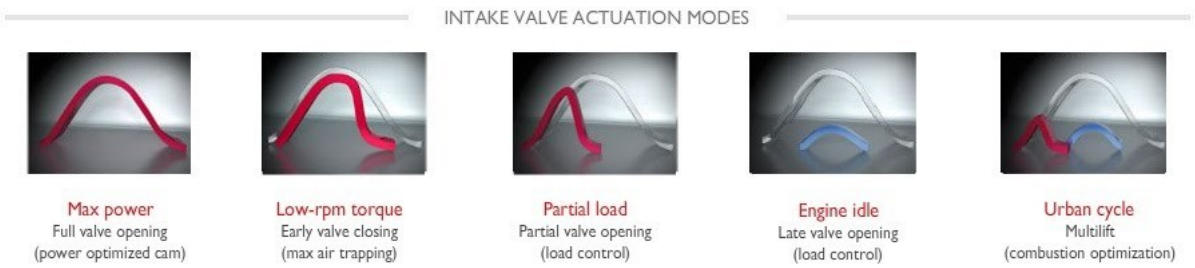

Figure 26 - Multiair characteristics (VVA by FCA)

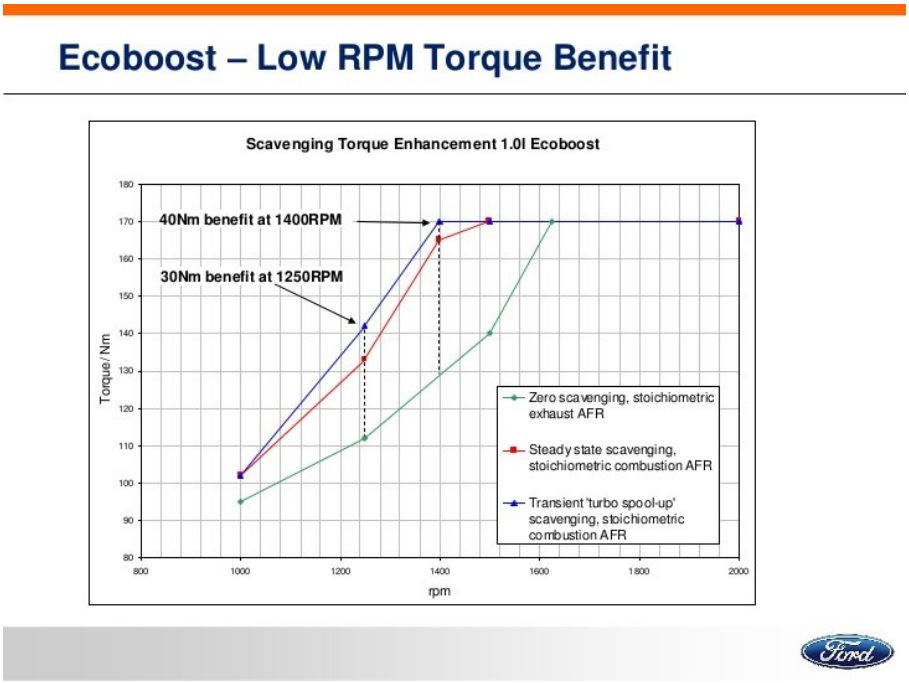

Figure 27 - Ecoboost and scavenging (Ford)

Another step they are taking is substituting the 5-speed gearboxes with 6-speed ones and even robotizing them or substituting them with DCT. The old automatic gearbox that once had no market segment in Europe, thanks to its penetration in sportiest variants and further adoption in lower segment is now one of the most requested by users (even if it doesn't have much in common with a torque converter automatic). The use of automatic gearboxes is particularly advantageous under the point of view of the WLTP homologation standard.

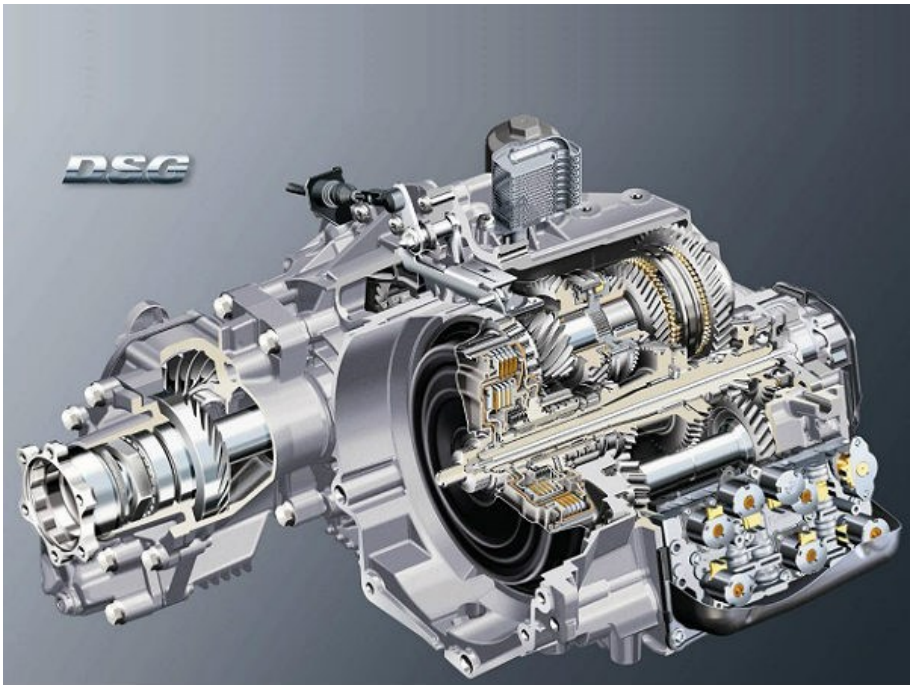

Figure 28 - 10 Speed Double Clutch Transmission (VW Group)

Other steps taken to reduce the fuel consumption and consequent CO2 emissions are the substitution of the classic starter with a more robust and prone to heavy duty cycles Start&Stop device that offers the added benefit of switching off during idles in traffic jams or at traffic lights. A further improvement of this concept comes from the BSG (Belt-Driven Starter Generator) that combines the starter with the alternator in a single electric machine and has the capability of driving in “pure electric” the ICE engine up to a certain speed, avoiding or reducing the cold cranking operation that are often responsible for obnoxious HC emissions, contemporarily storing part of the energy otherwise wasted during braking in the battery. Due to the added power required by the BSG often the electrical systems of modern cars require a Dual voltage (48, 60 or even 72 V) architecture alongside the old 12 V DC.

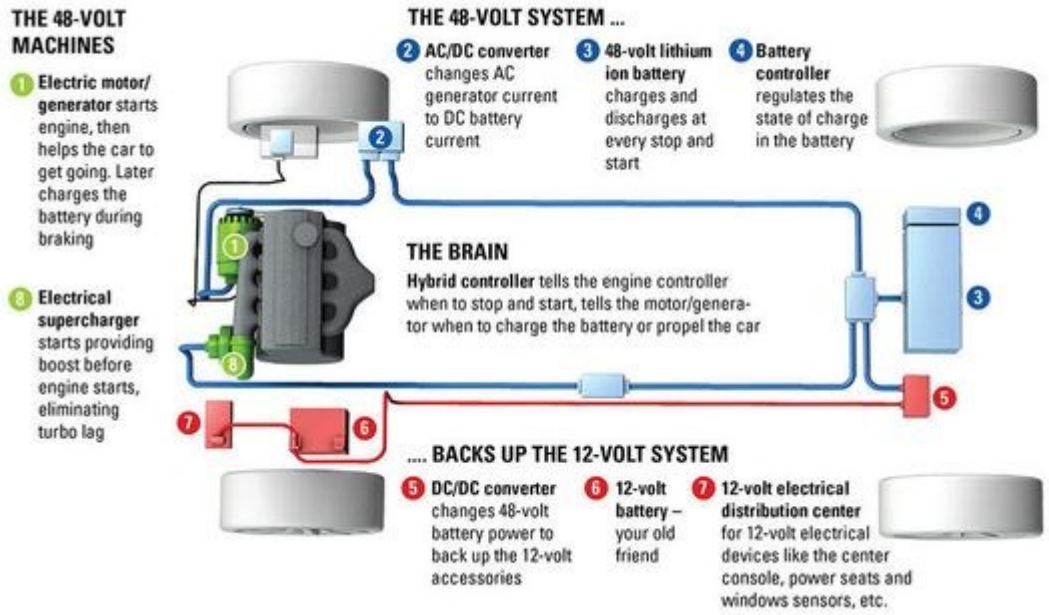

Figure 29 - Dual voltage architecture

The electrification is further increased by switching elements once fluid driven or mechanically coupled to the engine such as power steering and air conditioning to electrically actuated ones, even using electric switchable water pumps. It must be added also the benefit of dual loop thermal management system, with revised thermal engine architecture (e.g. exhaust headers integrals with the head) and careful considerations about radiators and thermal users optimized through the use of a single loop comprising the engine cooling, the intake air cooling, the EGR cooling and the air conditioning with the use of a single or a single set of modular Water/Air heat exchangers, can reach significant improvements in fuel

consumption reduction and weight reduction for the same performance, but this would be impossible without electrically actuated valves and pumps.

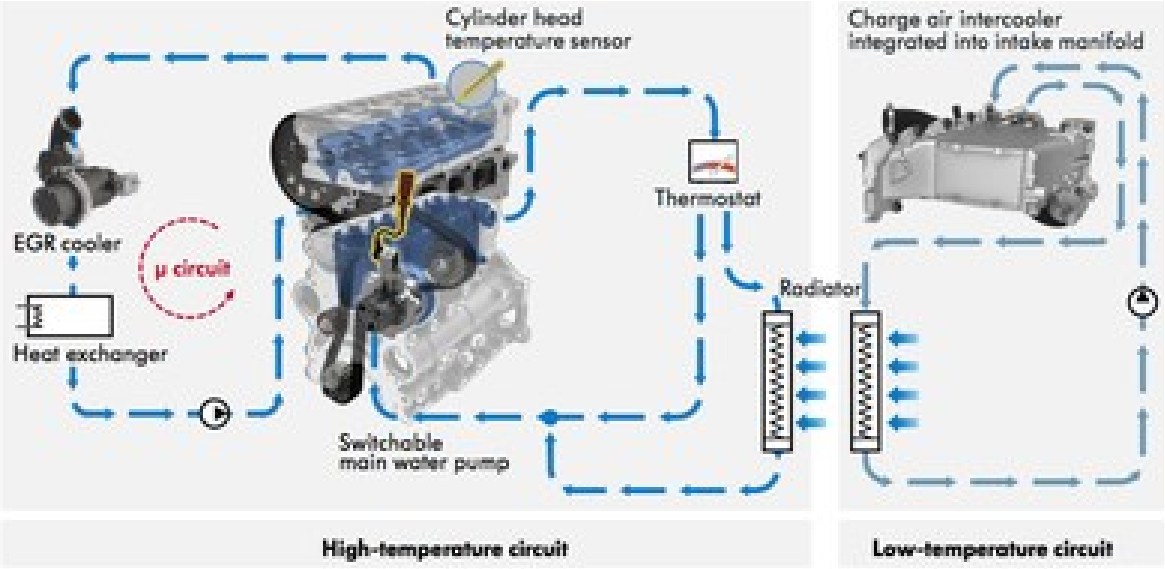

Figure 30 - Audi integrated and advanced cooling solution

During the past, and even today, some carmakers tried also to produce some models completely electric, to comply with the philosophy “Zero Emission Vehicle” but due to the immaturity of battery accumulators, especially in the past, it was not a viable solution (it maybe now with some caveats), mainly due to weight, range and charging time.

Figure 31 - Fiat Panda Elettra (1990)

2.3. The hybrid approach

So, the solution explored by some carmakers, Toyota in particular, was to exploit the benefits of both architecture (ICE and electric, thus hybrid) without pushing too much on the front of complete electrification but trying to tackle the biggest inefficiencies of the ICE. The combination of the best (but also economically viable) technology concerning the electrical powertrain and the strong integration with the ICE (even at the cost of dropping the turbocharging for size and economic constraints) allowed the Japanese carmaker to develop a medium sized sedan that with a small premium on the price could be marketed as environmentally friendly, building a user base for this product. The next step taken by Toyota was (while refining the architecture and concentrating on the single component) expanding in more market segments, the first of which was the luxury one with Lexus and its high end models (currently each model of Lexus sold in Europe come with at least an hybrid variant and ICE-only variants are the sportier model), and contemporarily populating also the mainstream and generalist brand of Toyota with hybrid powertrains in different market segments, as SUVs with the RAV4 (and the lather crossover C-HR) or station-wagon and hatchback with the Auris and even expanding in the subcompact (B) segment with the Yaris.

Figure 32 -2013 line-up of Toyota Hybrids

This rapid expansion and growth of hybrid vehicles (from 0 units to 10M in just ten years) would not be possible without the use of design concept of relatively recent creation in the automotive industry such as modularity and platform design. The THS II system is compact and modular and could be adapted to very different car segments.

Toyota Eco Project (January 1997):

- Prius on the Japanese market from December 1997: first passenger HEV for mass production
- THS (Toyota Hybrid System): hybrid powertrain based on the combination of a gasoline ICE and two e-drives. It is the first realisation of Toyota **Hybrid Synergy Drive (HSD)**
- in 2000 the second generation Prius (New Prius) is on the market Japanese market and from mid of the year is available first also in North America and then in Europe
- in 2003 Toyota reached 120.000 Prius (THS) sold worldwide
- from 2004 the Prius 2004 is on the global market with the THS II
- in May 2008 Toyota reached 1M Prius sold (315.000 in Japan and around 715.000 in the rest of the world (around 100.000 in Europe))
- from end of 2008 the third generation Prius is on the market
- Toyota and Lexus started to sell also lots of hybrid versions of ICE based vehicles. For instance: Toyota Camry, Highlander, Yaris and Auris Hybrid, Lexus RX400h, RX450h, GS450h, LS600h…
- Lexus put on the market also the CT200h and HS 250h (only hybrid)
- Toyota cumulatively sold in September 2009 2M hybrids (Toyota and Lexus)
- in September 2010 Toyota cumulatively sold 2M Prius
- from the end of 2011 the Prius P-HEVs is on the market
- in 2012 Toyota-Lexus sold around 1,2M hybrids
- Toyota cumulatively (Toyota and Lexus) sold:
  - 5M hybrids (March 2013)
  - 7M hybrids (October 2014)
  - 8M hybrids (August 2015)
  - 9M hybrids (April 2016)
- in November 2015 new Prius has been presented (Tokyo Motor Show) first with New TNGA (Toyota New Global Architecture)
- in December 2015 Toyota cumulatively sold 1M hybrids in Europe
- In April 2016 Toyota cumulatively sold 1M Lexus hybrids
- Hybrid vehicles sales target of 1.5 million units annually and 15 million units cumulatively by 2020 announced in Toyota Environmental Challenge 2050

Figure 33 - Milestones in Hybrid Electric Vehicles development and sales by Toyota

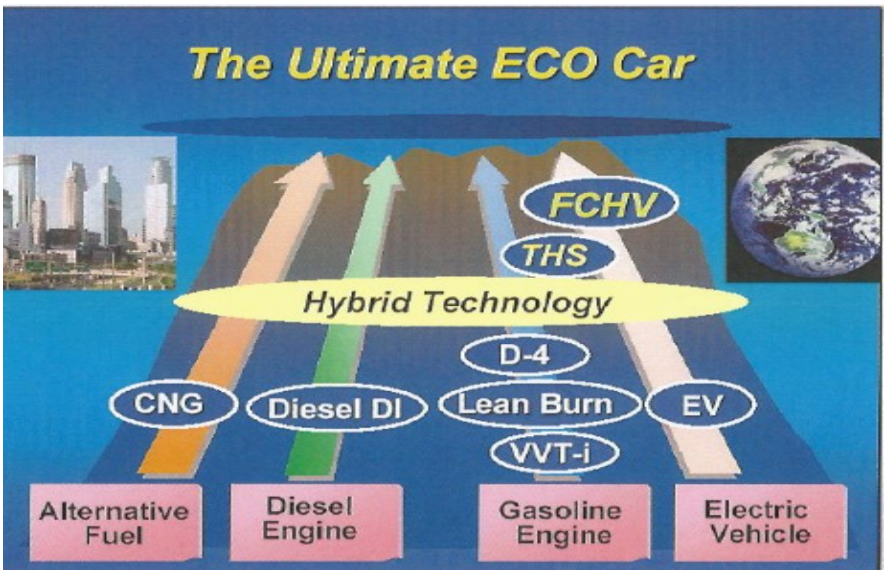

Figure 34 - - The Ultimate ECO Car (Toyota philosophy)

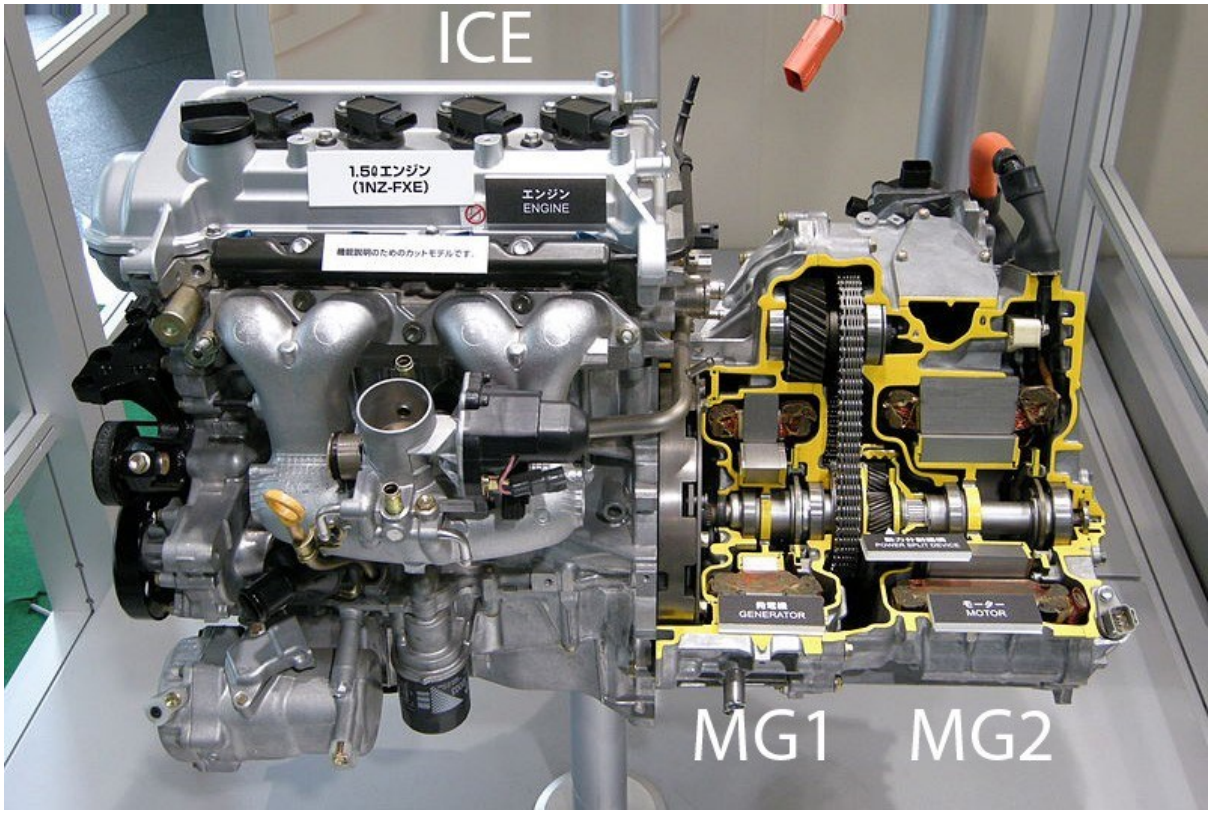

Figure 35 - THS II by Toyota: ICE, Generator CVT and Motor

It is also more efficient than the previous powertrain generation and in the context of Toyota Production Systems is continuously improved at each revision.

The current system is composed by an ICE engine and 2 electric machines coupled to it through a multistage shifter, in order to obtain the maximum efficiency from each component widening the operating point of the two electric machines. The entire system is coupled to a CVT capable of simulating a 10-speed gearbox. Every electric machine is an AC brushless one with a PCU (Power Control Unit) comprised of an inverter and a Buck/Boost converter. Its batteries are NiMH or Li-Ion adding the possibility of a Plug-in variant.

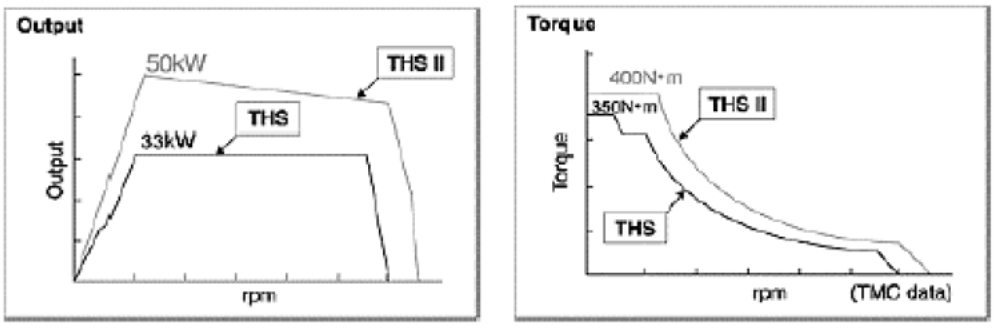

Fig. 2. Comparison of output power and torque versus speed between 2003 (THS) and 2004 (THS II) Prius motor.

Figure 36 - Comparison between THS and THS II

Toyota Hybrid THS II

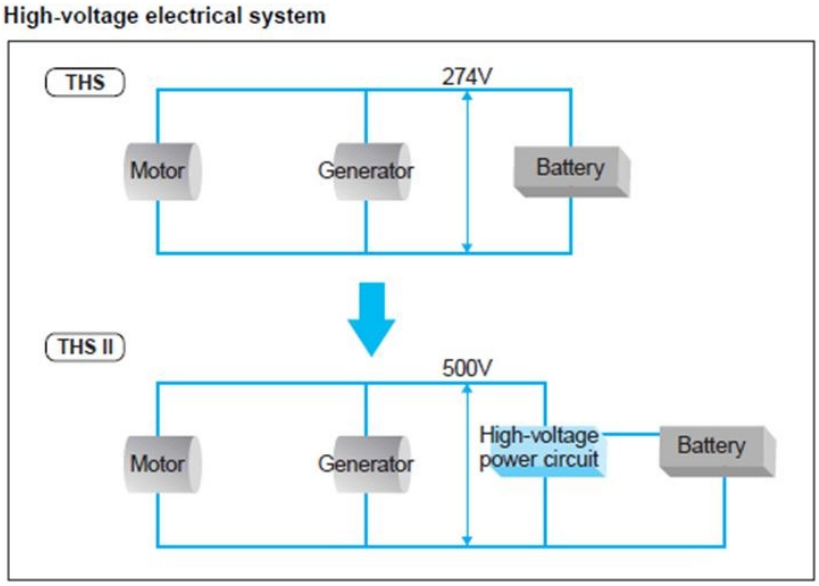

Figure 37 - THS II electronic architecture

One of the most interesting feature of the new THS system presented in 2016 is the possibility (already implemented with the RAV4 and some other SUVs, crossover and minivans) of coupling a rear-axle electric motor giving the capability of 4WD, making the architecture a Split Series-Parallel Hybrid at the front and a P4 at the rear, through the use of a single PCU managing all the 3 different electric machines.

4WD Hybrids are of particular interests for many carmakers for multiple reason. First, 4WD is usually fitted to premium vehicles or at least high-end variants of mainstream models, so the complexity and engineering costs could be easily balanced by the premium in the final price paid by the client. Secondly 4WD is mainly fitted on some segments as SUVs, Minivans and Crossovers, that both in Europe (except for Minivans) and NAFTA regions have seen a conspicuous rise in the last 15 years (figures 38 and 39) to the point that J-segments and M-segments now follow the subdivision of A-E segments in Europe.

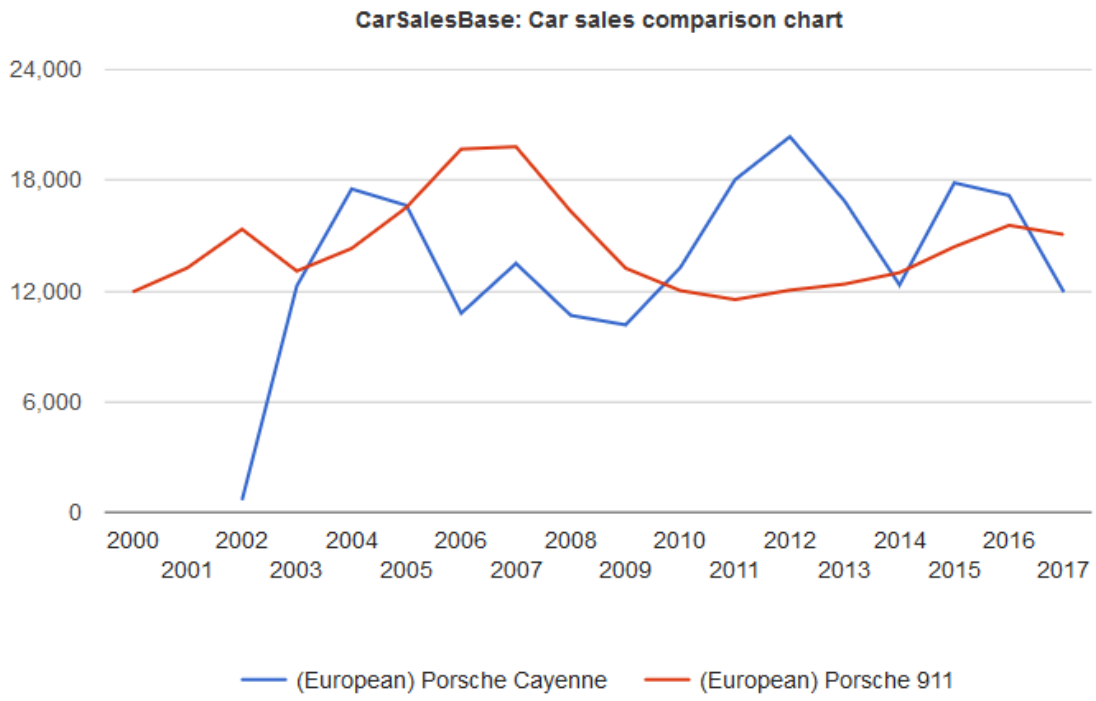

Figure 38 - Sales of Porsche Cayenne VS 911 in Europe

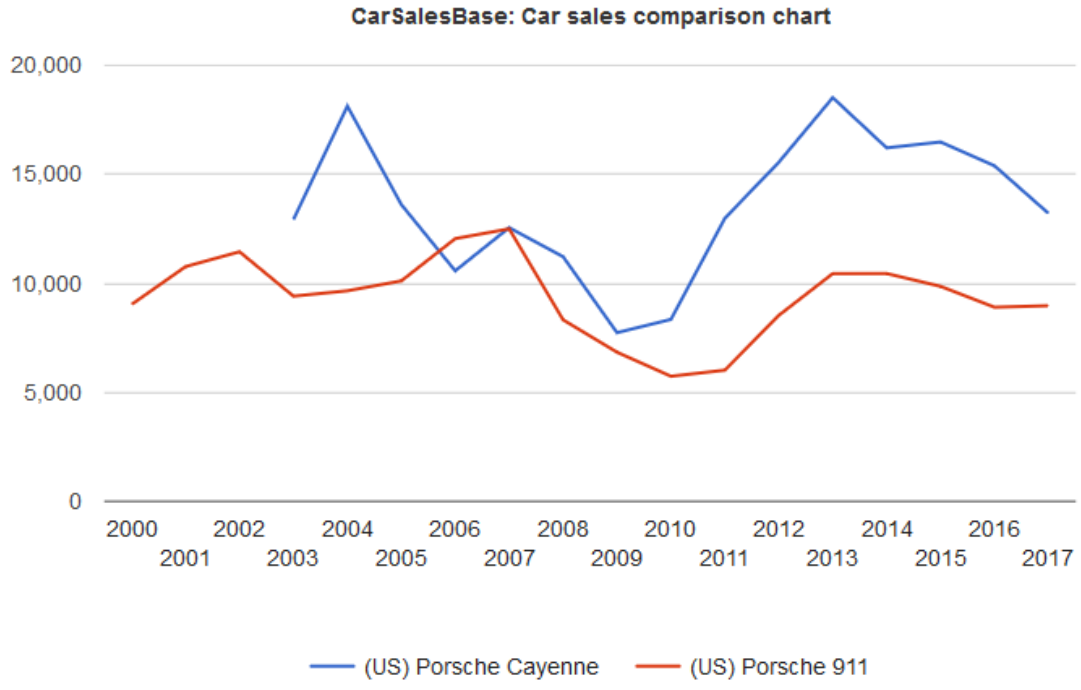

Figure 39 - Sales of Porsche Cayenne VS 911 in USA

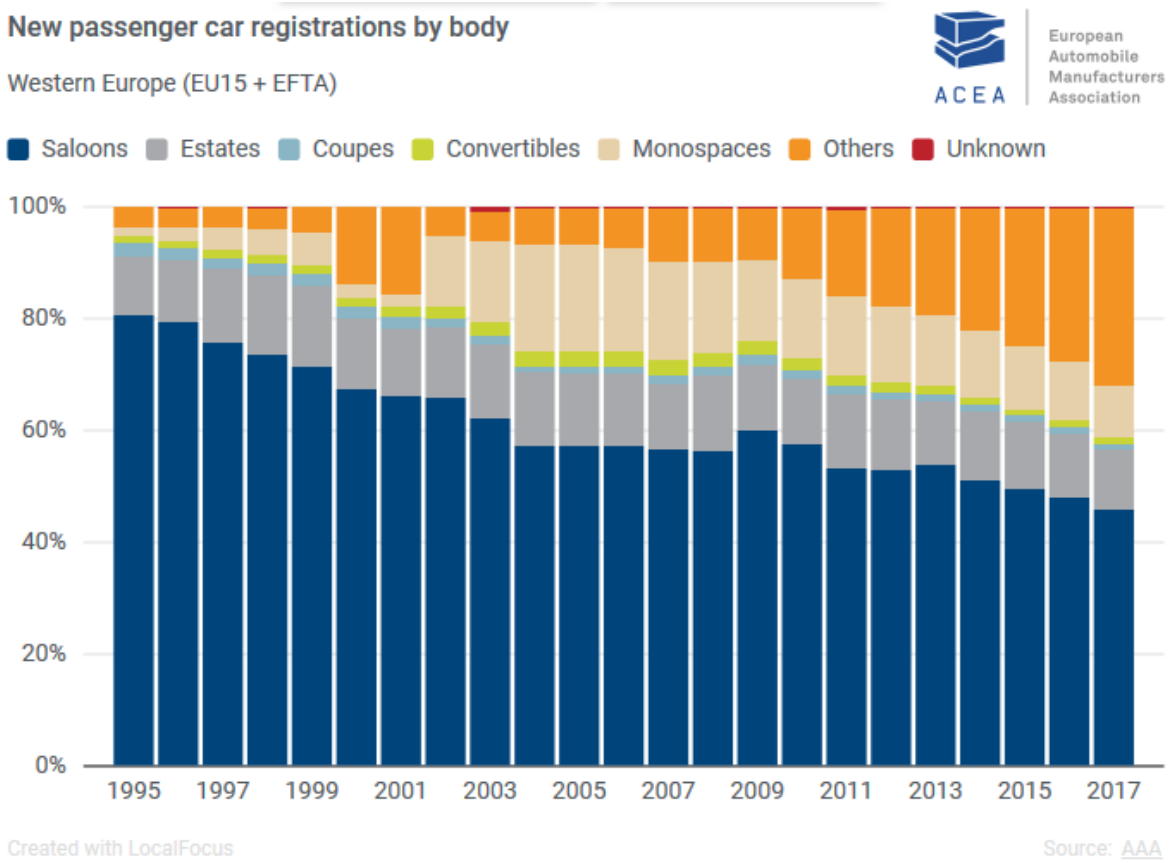

Figure 40 - Passenger car registration by body (ACEA, 2017)

Furthermore, these vehicles, despite having seen a conspicuous rise in sales, are the heaviest and consequently the ones with the highest fuel consumption and CO2 emission. So, for a carmaker that wants both to maintain a strong position in these high-revenue segments while contemporarily reducing the fleet emission in order to not incur in the heavy fines for exceeding the fleet limits set by EU commission and CAFE standards, it is vital to lower the emissions of the highest emitting vehicles, the J and M segments car in particular. Since the two best-selling subsegments are currently (according to sales figures of 12/2017) the B-SUV and C-SUV ones, and since many SUV variants are developed from the standard B, C or D platforms, is logical to start from them, and when the product is mature and the learning curve has been climbed, transfer the powertrain architecture to the non-SUV segments that have highest volumes but lower revenues per vehicle, so are not so convenient for launching new technologies.

The 4WD Hybrid offer also some capabilities not offered by the standard FWD Hybrid. For example, the start of the car in full electric mode without any loss due to the mechanical movement of the ICE engine even if in not firing condition, not attainable in configuration other than P3 or some P2 variants. With the rear axle controlled by an electric motor, even if there is still a mechanical differential

between it and the wheels, the traction could be managed much more efficiently and without the loss connected to limited slip differentials or the complexity of some of their variants and its relative weight. The elimination of the mechanical link between the two axles makes sufficient room to stuff the HV battery in the central underside portion of the vehicle, thus improving the weight distribution between the axles and lowering the centre of gravity of these J and M segments vehicles, notoriously high. It must be noted that the lowering of the centre of height is not due to a relocation of existing masses but effectively to the addition of these new masses, since Hybrid variants are significantly heavier than their pure ICE counterparts, due to their system complexity and HV batteries in particular. But this weight increase is heavily compensated in terms of performances by the electric power added by the electric engine, especially the instant torque at the lower regimes.

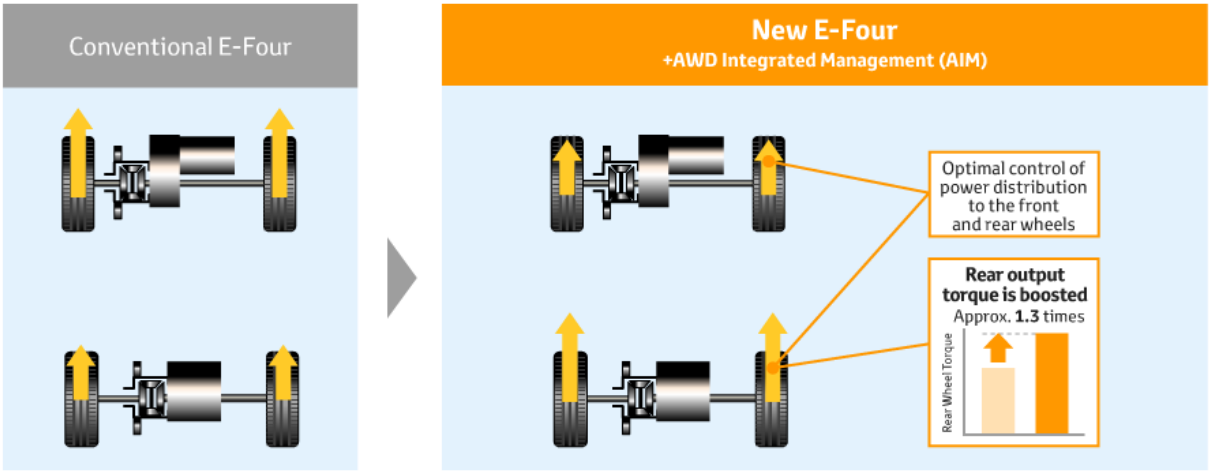

Figure 41 - 4WD Hybrid system by Toyota

The electro-mechanic configuration permits also to harvest power from the rear axle during braking, thus recharging the HV battery with an higher efficiency when compared to P1/P2 configuration, even if due to the nose dip/tilt connected to the braking momentum the harvestable power at the rear axle is limited, but in combination with the electric machine at the front is a good compromise for the regenerative braking. The presence of the P1/P2 electric machine at the front, being before the gearbox, and if the P2 EM is detachable from the gearbox through a devoted clutch but still attachable to the ICE engine, it gives the capability of a series hybrid to the vehicle, with the ICE generating power, converted by the front EM in electricity, then transferred to the rear EM (and even some fraction to the HV battery). For the impossibility (or the impracticality) of applying this control strategy and for the inconvenience of having the front EM with a fixed transmission

ratio with respect to the front wheels, the P3 configuration in this 4WD Hybrid system is not viable. The parallel hybrid configuration is rather obvious, while the full electric configuration could be attained in different modes and with different efficiencies. Regarding the front section of the powertrain the 3 viable configurations are substantially P1f, P1r and P2. While the last could theoretically be the most efficient it is also the most complex to correctly develop, due to an added clutch and the needs of modifying the gearbox to accommodate the solution, it is not a good solution to accommodate in an existing platform using existing gearboxes and ICE. The P1r has similar problems, because, even if some modification to the ICE is necessary and often convenient, accommodating the electric motor in the neighbourhood of the flywheel is still problematic without heavily revising the flywheel side of the engine (although it can be used as a replacement for the starter). But if the case is an existing (or not exclusive or purpose-built) ICE, the most convenient thing is to use a BAS with a pretensioner mechanism that permits to vary the tension applied to the belt and thus varying the transmission ratio.

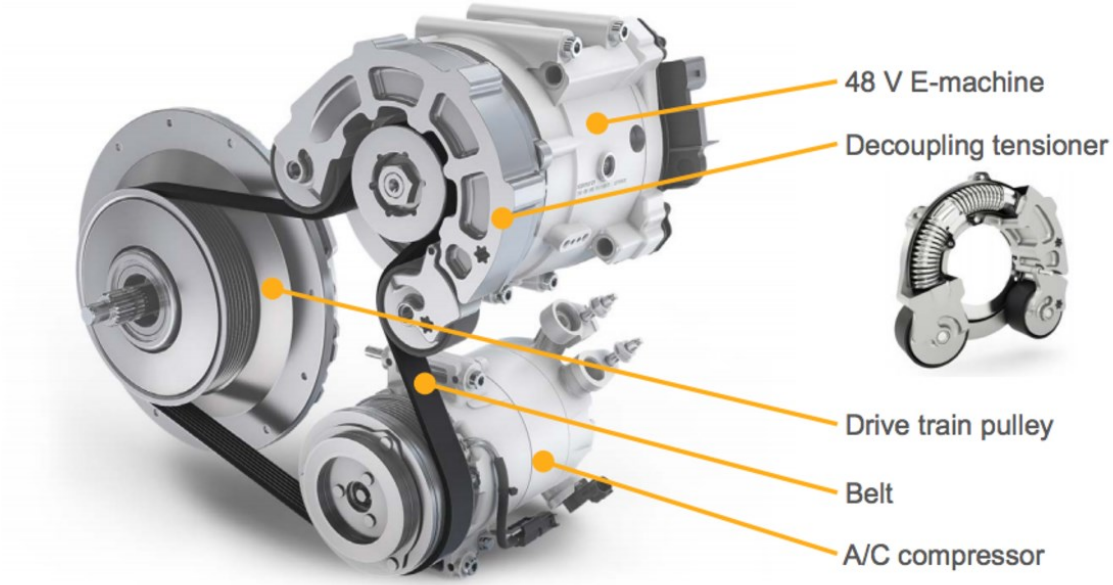

Figure 42 - BAS with variable tensioner

The full electric capability of the 4WD hybrids (and of hybrids in general) is very interesting from the point of view of homologation since it permits to complete homologation test cycles if correctly designed and lower substantially the emitted emission. For instance, several plug-in hybrid cars homologated during the NEDC cycle thanks to definition contained in the regulation 83 of UNECE, could declare

very low CO2 emission (in the neighbourhood of 40-50 g/km) and combined fuel consumption (around 1.5-2.5 l/100 km, while most declare 0 for the Urban and Extra Urban part). This problem of “fake” fuel consumption and CO2 emission is more correctly addressed in the WLTP test procedure, but still manufacturers, even according to some academic sources, have the possibility to fine tune their strategy for homologation. Furthermore, a correct sizing of EMS strategies and hybrid control strategies in the switch from NEDC to WLTP procedures could lead to a reduced electric range (thus more realistic) but oddly to a possible decrease in CO2 emissions (Jelica Pavlovic). It must be noted that Vehicle 2 is a parallel hybrid variant of a vehicle born as a pure EV (often called range extended) so this behaviour is largely expectable.

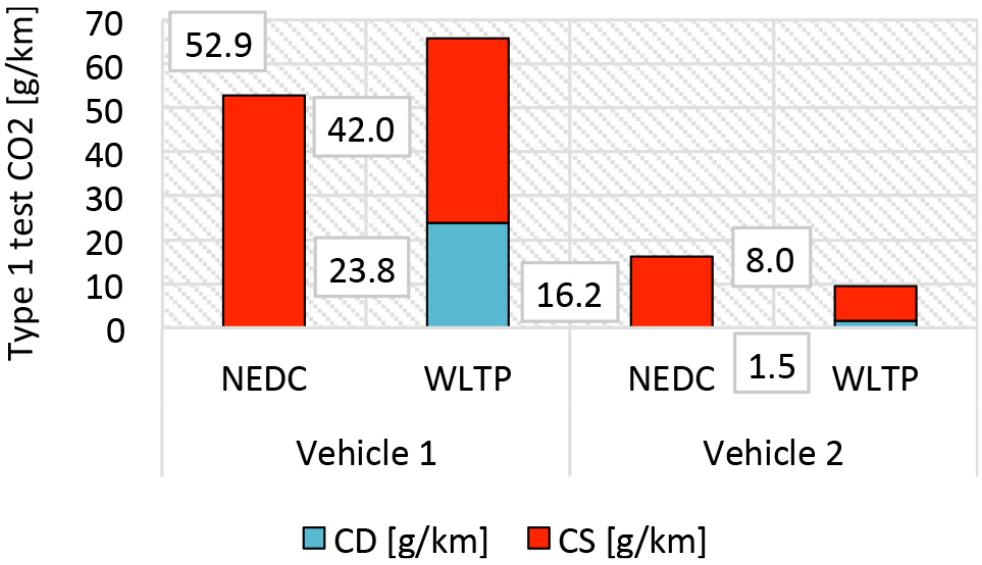

Figure 43 - NEDC and WLTP tests of two HEV

3. Regulation compliance of Hybrid Vehicles

3.1. NEDC and double testing

Developing a vehicle or a variant that could be marketed within 2021 will require to consider the double testing of NEDC and WLTP. The test procedures differ greatly also from the point of view of the Hybrid Electric emissions, fuel consumption and electric range. NEDC didn't provide any electric range (while EPA does) but had a different mode of considering fuel consumption subdividing in Urban Cycle, Extra-Urban Cycle and Combined. Vehicles capable of executing at least a full NEDC cycle (consisting of four Urban Cycles and one Extra-Urban Cycle) in full electric mode without ever switching on the ICE, would result in a 0 l/100 km for the first two part. In order to prevent a 0 l/100 km in the mixed cycle and 0 g/km emission the regulation 101 of the E/ECE/TRANS/505 provided a strategy for calculating the Fuel Consumption of HEV vehicles, especially Plug-In ones with switchable modes.

The HEV OCV with switchable mode selection is considered. It distinguishes two cases: starting from a full charge and starting from the minimum admissible charge after a preconditioning. These two cases are called in the WLTP Charge Depleting and Charge Sustain, while in the regulation 101 as Condition A and B.

Hybrid-modes / *Battery state of charge*	*Pure electric Hybrid* — *Switch in position*	*Pure fuel consuming Hybrid* — *Switch in position*	*Pure electric Pure fuel consuming Hybrid* — *Switch in position*	*Hybrid mode n* ... Hybrid mode m** — *Switch in position*
Condition A Fully charged	Hybrid	Hybrid	Hybrid	Most electric hybrid mode**
Condition B Min. state of charge	Hybrid	Fuel consuming	Fuel consuming	Most fuel consuming mode***

* For instance: sport, economic, urban, extra-urban position ...

** Most electric hybrid mode:

The hybrid mode which can be proven to have the highest electricity consumption of all selectable hybrid modes when tested in accordance with condition A, to be established based on information provided by the manufacturer and in agreement with the technical service.

*** Most fuel consuming mode:

The hybrid mode which can be proven to have the highest fuel consumption of all selectable hybrid modes when tested in accordance with condition B, to be established based on information provided by the manufacturer and in agreement with the technical service.

Figure 44 - Guidelines for mode selection (ECE R83)

Regarding Condition B the vehicle is preconditioned in the subsequent way: “The electrical energy/power storage device of the vehicle is discharged while driving with the switch in pure electric position (on the test track, on a chassis dynamometer, etc.) at a steady speed of 70 per cent ± 5 per cent of the maximum speed of the vehicle in pure electric mode” and “Stopping the discharge occurs:

(a) When the vehicle is not able to run at 65 per cent of the maximum 30 minutes speed; or

(b) When an indication to stop the vehicle is given to the driver by the standard on-board instrumentation; or

(c) After covering a distance of 100 km.

If the vehicle is not equipped with a pure electric mode, the electrical energy/power storage device discharge shall be achieved by driving the vehicle (on the test track, on a chassis dynamometer, etc.):

(a) At a steady speed of 50 km/h until the fuel consuming engine of the HEV starts up;

(b) Or if a vehicle cannot reach a steady speed of 50 km/h without starting up the fuel consuming engine, the speed shall be reduced until the vehicle can run a lower steady speed where the fuel consuming engine just does not start up for a defined time/distance (to be specified between technical service and manufacturer);

(c) Or with manufacturer's recommendation.

The fuel-consuming engine shall be stopped within ten seconds of it being automatically started.”

In this way, after having selected the most fuel consuming hybrid mode the vehicle undergoes a NEDC cycle. Subsequently it is fully recharged and fully discharged again in order to measure the variation of electrical energy in the cycle and in case of non OCV HEV it could be applied some correction.

Regarding the Condition A the same procedure is applied (but after the initial conditioning the battery is charged), the most electric consumptive electric mode is selected (although not fully electric) and it could be chosen to execute a NEDC cycle (4.2.4.2.1) or to take the battery to full discharge (4.2.4.2.2). The second option introduce the break-off criteria of 3% variation in nominal capacity of the battery.

The SOC profiles for OVC-HEVs tested under conditions A and B are:

Condition A:

Figure 45 - Condition A test cycle

(1) Initial state of charge of the electrical energy/power storage device

(2) Discharge according to paragraph 3.2.1. or 4.2.2. of this annex

(3) Vehicle conditioning according to paragraphs 3.2.2.1./3.2.2.2. or 4.2.3.1./4.2.3.2. of this annex

(4) Charge during soak according to paragraphs 3.2.2.3. and 3.2.2.4. or 4.2.3.3. and 4.2.3.4. of this annex

(5) Test according to paragraph 3.2.3. or 4.2.4. of this annex

(6) Charging according to paragraph 3.2.4. or 4.2.5. of this annex

Condition B:

Figure 46 - Condition B test cycle

(1) Initial state of charge

(2) Vehicle conditioning according to paragraph 3.3.1.1. or 4.3.1.1. (optional) of this annex

(3) Discharge according to paragraph 3.3.1.1. or 4.3.1.1. of this annex

(4) Soak according to paragraph 3.3.1.2. or 4.3.1.2. of this annex

(5) Test according to paragraph 3.3.2. or 4.3.2. of this annex

(6) Charging according to paragraph 3.3.3. or 4.3.3. of this annex

(7) Discharging according to paragraph 3.3.4. or 4.3.4. of this annex

(8) Charging according to paragraph 3.3.5. or 4.3.5. of this annex

The two emission modes are then combined according to section 4.4.

4.4 Test results

4.4.1. The values of CO2 shall be M1 = m1/Dtest1 and M2 = m2/Dtest2 (g/km) with Dtest1 and Dtest2 the total actual driven distances in the tests performed under conditions A (paragraph 4.2. of this annex) and B (paragraph 4.3. of this annex) respectively, and m1 and m2 determined in paragraphs 4.2.4.5. and 4.3.2.5. of this annex respectively.

4.4.2 The weighted values of CO2 shall be calculated as below:

4.4.2.1.In the case of testing according to paragraph 4.2.4.2.1. of this annex: M = (De·M1 + Dav·M2)/(De + Dav)

Where:

M = mass emission of CO2 in grams per kilometre.

M1 = mass emission of CO2 in grams per kilometre with a fully charged electrical energy/power storage device.

M2 = mass emission of CO2 in grams per kilometre with an electrical energy/power storage device in minimum state of charge (maximum discharge of capacity).

De = vehicle's electric range, according to the procedure described in Annex 9 to this Regulation, where the manufacturer must provide the means for performing the measurement with the vehicle running in pure electric operating state.

Dav = 25 km (assumed average distance between two battery recharges).

4.4.2.2. In the case of testing according to paragraph 4.2.4.2.2. of this annex:

M = (Dovc·M1 + Dav·M2)/(Dovc + Dav)

Where

M = mass emission of CO2 in grams per kilometre.

M1 = mass emission of CO2 in grams per kilometre with a fully charged electrical energy/power storage device.

M2 = mass emission of CO2 in grams per kilometre with an electrical energy/power storage device in minimum state of charge (maximum discharge of capacity).

Dovc = OVC range according to the procedure described in Annex 9 to the Regulation.

Dav = 25 km (assumed average distance between two battery recharges).

4.4.3. The values of fuel consumption shall be:

C1 = 100·c1/Dtest1 and C2 = 100·c2/Dtest2 (l/100 km)

with Dtest1 and Dtest2 the total actual driven distances in the tests performed under conditions A (paragraph 4.2. of this annex) and B (paragraph 4.3. of this annex) respectively, and c1 and c2 determined in paragraphs 4.2.4.5. and 4.3.2.5. of this annex respectively.

4.4.4. The weighted values of fuel consumption shall be calculated as below:

4.4.4.1. In the case of testing according to paragraph 4.2.4.2.1. of this annex:

C = (De·C1 + Dav·C2)/(De + Dav)

Where:

C = fuel consumption in l/100 km.

C1 = fuel consumption in l/100 km with a fully charged electrical energy/power storage device.

C2 = fuel consumption in l/100 km with an electrical energy/power storage device in minimum state of charge (maximum discharge of capacity).

De = vehicle's electric range, according to the procedure described in Annex 9 to this Regulation, where the manufacturer must provide the means for performing the measurement with the vehicle running in pure electric operating state.

Dav = 25 km (assumed average distance between two battery recharges).

4.4.4.2. In the case of testing according to paragraph 4.2.4.2.2. of this annex:

C = (Dovc·C1 + Dav·C2)/(Dovc + Dav)

Where:

C = fuel consumption in l/100 km.

C1 = fuel consumption in l/100 km with a fully charged electrical energy/power storage device.

C2 = fuel consumption in l/100 km with an electrical energy/power storage device in minimum state of charge (maximum discharge of capacity).

Dovc = OVC range according to the procedure described in Annex 9 to this Regulation.

Dav = 25 km (assumed average distance between two battery recharges).

4.4.5. The values of electric energy consumption shall be:

E1 = e1/Dtest1 and E4 = e4/Dtest2 (Wh/km)

With Dtest1 and Dtest2 the total actual driven distances in the tests performed under conditions A (paragraph 4.2. of this annex) and B (paragraph 3.3. of this annex) respectively, and e1 and e4 determined in paragraphs 4.2.6. and 4.3.6. of this annex respectively.

4.4.6. The weighted values of electric energy consumption shall be calculated as below:

4.4.6.1. In the case of testing according to paragraph 4.2.4.2.1.:

E = (De·E1 + Dav·E4) / (De + Dav)

Where:

E = electric consumption Wh/km.

E1 = electric consumption Wh/km with a fully charged electrical energy/power storage device calculated.

E4 = electric consumption Wh/km with an electrical energy/power storage device in minimum state of charge (maximum discharge of capacity).

De = vehicle's electric range, according to the procedure described in Annex 9 to this Regulation, where the manufacturer must provide the means for performing the measurement with the vehicle running in pure electric operating state.

Dav = 25 km (assumed average distance between two battery recharges).

4.4.6.2. In the case of testing according to paragraph 4.2.4.2.2. of this annex:

E = (Dovc·E1 + Dav·E4) / (Dovc + Dav)

Where:

E = electric consumption Wh/km.

E1 = electric consumption Wh/km with a fully charged electrical energy/power storage device calculated.

E4 = electric consumption Wh/km with an electrical energy/power storage device in minimum state of charge (maximum discharge of capacity).

Dovc = OVC range according to the procedure described in Annex 9 to this Regulation.

Dav = 25 km (assumed average distance between two battery recharges).

It must be noted that in both 4.4.4.1 and 4.4.4.2, C1 could be 0 and the more the electric range is, calculated in one of the two ways, is significantly reducing and affecting the fuel consumption of the Condition B. The same holds for CO2 emissions.

3.2. WLTP procedure for OCV-HEV vehicles

The WLTP tests for OCV-HEV Vehicles are similar, with the introduction of electric range but substantially maintaining the two kinds of testing (CS and CD).

Table A6/1

Applicable rules for a manufacturer's declared values (total cycle values) (1)

Vehicle type		M_{CO2} (2) (g/km)	FC (kg/100 km)	Electric energy consumption (3) (Wh/km)	All electric range / Pure Electric Range (3) (km)
Vehicles tested according to Sub-Annex 6 (ICE)		M_{CO2} Paragraph 3. of Sub-Annex 7	—	—	—
NOVC-FCHV		—	FC_{CS} Paragraph 4.2.1.2.1. of Annex 8	—	—
NOVC-HEV		$M_{CO2,CS}$ Paragraph 4.1.1. of Sub-Annex 8	—	—	—
OVC-HEV	CD	$M_{CO2,CD}$ Paragraph 4.1.2. of Sub-Annex 8	—	$EC_{AC,CD}$ Paragraph 4.3.1. of Sub-Annex 8	AER Paragraph 4.4.1.1. of Sub-Annex 8
	CS	$M_{CO2,CS}$ Paragraph 4.1.1. of Sub-Annex 8	—	—	—
PEV		—	—	EC_{WLTC} Paragraph 4.3.4.2. of Sub-Annex 8	PER_{WLTC} Paragraph 4.4.2. of Sub-Annex 8

The OCV-HEV vehicle could be tested in 4 variants, but the less time-consuming and thus more cost-effective is the CD+CS variant (option 3).

Figure A8/1

Possible test sequences in the case of OVC-HEV testing

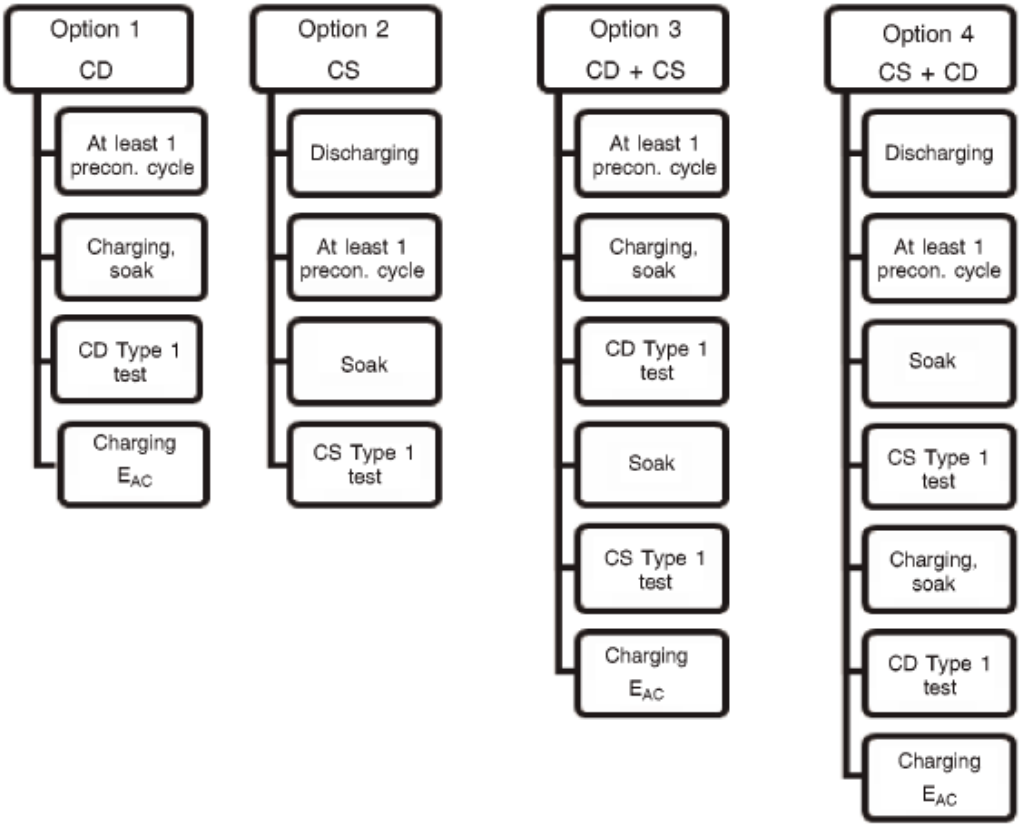

Figure 47 - Test sequence for OVC-HEV testing according to WLTP

The driver-selectable mode must be chosen according to the flowchart exposed in the regulation at the Annex XXI Sub annex 8 Appendix 6, Paragraphs 2 and 3.

Figure A8.App6/1

Selection of driver-selectable mode for OVC-HEVs under charge-depleting operating condition

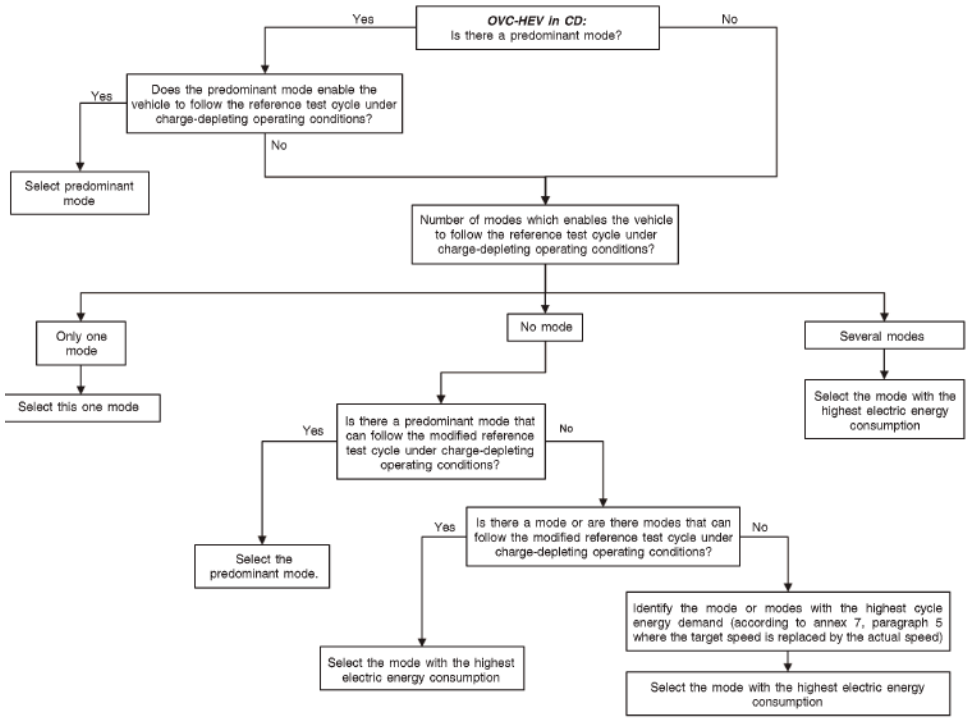

Figure 48 -WLTP Charge Depleting flow-chart

Figure A8.App6/2

Selection of a driver-selectable mode for OVC-HEVs, NOVC-HEVs and NOVC- FCHVs under charge-sustaining operating condition

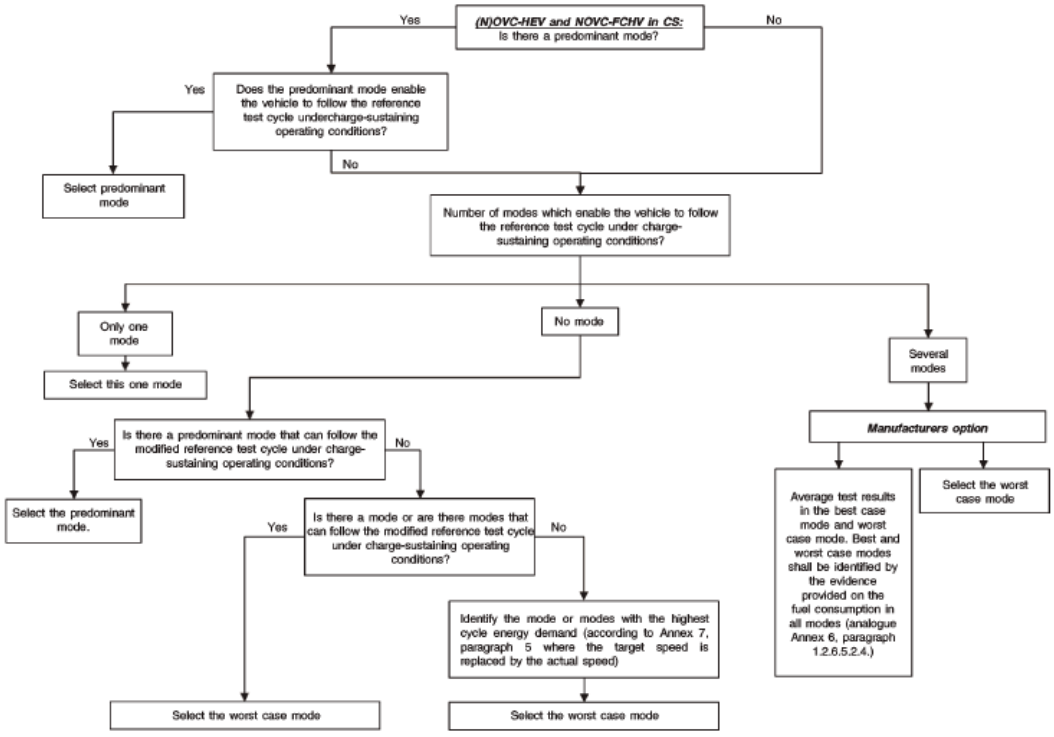

Figure 49 - WLTP Charge Sustaining flow-chart

The CD cycle is similar to the 4.2.4.2.2 variants of the NEDC. Multiple (n) WLTC are executed until the variation of energy in the accumulators is less than 4% the calculated (using Paragraph 5, Sub annex 7 of the same Annex) energy expended during a WLTC run of the test vehicle. Then another WLTC run (n+1) is executed, called the confirmation cycle, in order to confirm that the accumulators are entirely discharged. Only the n cycles are considered. The energy variation is directly and constantly monitored on the REESS integrating the instant current and voltage measured through and on it, rather than dealing with the less precise capacity monitoring, becoming imprecise with Li-Ion batteries that presents a non-linear behaviour in discharge.

The CS cycle is a simple WLTC run with the battery theoretically discharged, thus the convenience of executing it after the CD cycle.

The true novelty of the WLTP procedure is how the emissions and fuel consumption are calculated (other than the electric range). Being it the most critical for the CO2 emission fleet standard is important to understand the mechanism.

First of all it is possible to account for multiple correction, e.g. if during the Charge Depleting cycle the REESS are recharged (during the last part of the EH sub cycle of the WLTC there is a strong brake to an halt that could be used to harvest energy) the excess of electrical energy could be "traded" for CO2 emitted during the cycle (the variation is usually pretty small, in the order of 1-2% maximum). Secondly the combination of CD and CS cycle are different, due to the Utility Factors. They are present in the WLTP regulation as a concept, but the precise values are left to the local legislators. The EU ones are depicted in table 4 according to the equation below

$$UF_i(d_i) = 1 - \exp\left(-\left(\sum_{j=1}^{k} C_j \times \left(\frac{d_i}{d_n}\right)^j\right)\right) - \sum_{l=1}^{i-1} UF_l$$

Where:

UF_i Utility factor for phase i.

d_i Distance driven to the end of phase i in km.

C_j j^{th} coefficient (see Table 4).

d_n Normalized distance (see Table 4).

k Amount of terms and coefficients in the exponent see Table 4).

i Number of considered phase.

j Number of considered term/coefficient.

$\sum_{l=1}^{i-1} UF_l$ Sum of calculated utility factors up to phase (i-1).

The curve that is based on the following parameters in Table 4 is valid from 0 km to the normalized distance d_n where the UF converges to 1.0 (as can be seen in Figure 50).

C_1	26,25
C_2	– 38,94
C_3	– 631,05
C_4	5 964,83
C_5	– 25 094,60
C_6	60 380,21
C_7	– 87 517,16
C_8	75 513,77
C_9	– 35 748,77
C_{10}	7 154,94
d_n [km]	800
k	10

Table 4 - Utility Factor Parameter from EU regulations

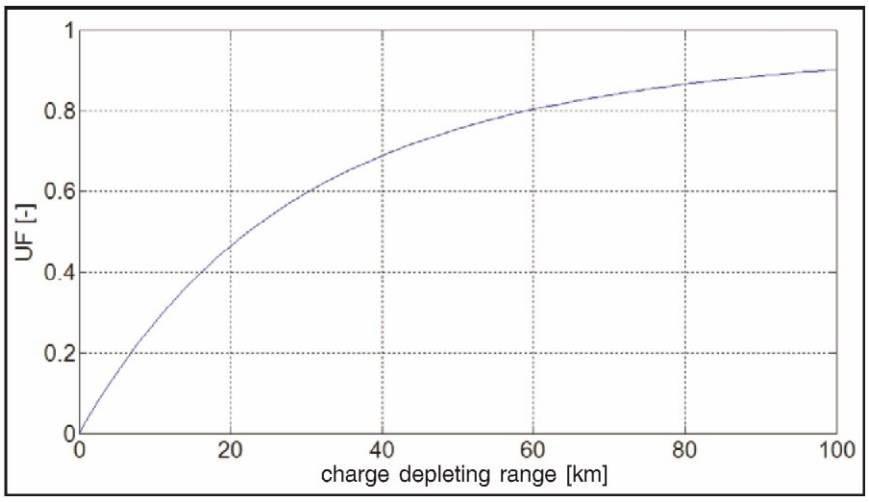

Figure 50 - Utility Factor curve based on equation parameter of Table 4

The equation for calculating the combined emission is:

$$M_{i,weighted} = \sum_{j=1}^{k}(UF_j \times M_{i,CD,j}) + (1 - \sum_{j=1}^{k} UF_j) \times M_{i,CS}$$

Where Mi,CD,j are the emissions for each of the Charge Depleting cycle from 1 to k and Mi,CS the emissions for the Charge Sustaining one.

It is easily noticeable that even in this case the electric range in CD mode is predominant, and it is by a greater extent, thus favouring large Plug-In hybrids over Mild hybrids. After 80 km of full electric range in CD mode the contribution of the Charge Sustain mode is practically less than 15% of the emission.

3.3. Development of a Matlab model for simulating the WLTC

In order to simulate both a NEDC scenario and a WLTP one a specific Matlab model composed of 4 subroutines has been implemented. The main script is the following:

```
en_type='';
gbx_type='';
fm_type='';
rm_type='';
bat_type='';
veh='';
cy='WLTP';
brake_off_p=4;


pwt=S1_Powertrain_generator(en_type,gbx_type,fm_type,rm_type,bat_type);

preq=S2_Cycle_P_req(veh,cy,pwt);
```

```
load(preq);
load(pwt, 'bat');

cd_cycle=sprintf("CD cycle %s",preq);
cs_cycle=sprintf("CS cycle %s",preq);

%% WLTP
% Charge depleting cycle
bat_cap=bat.max_cap;
cd=struct; cd.brake_off_c=0; j=1; d_s=0;
while (cd.brake_off_c(j)<=2)
    hy=S3_Powertrain_logic(pwt,preq,bat_cap,d_s);
    if (cd.brake_off_c(j)<2)
        if (((abs(hy.bat_en(end)-hy.bat_en(1))/(E_cycle/3.6*10^-
6))<brake_off_p/100))
            cd.brake_off_c(j+1)=cd.brake_off_c(j)+1;
        else
            cd.brake_off_c(j+1)=cd.brake_off_c(j);
        end
        commandLine = sprintf('cd.cycle%d = hy;', j);
        eval(commandLine);
    else
        break
    end
    j=j+1;
    bat_cap=hy.bat_en(end);
    d_s=hy.d(end);
end
save (cd_cycle,'cd');

% Charge sustaining cycle
bat_cap=hy.bat_en(end);
d_s=0;
cs=S3_Powertrain_logic(pwt,preq,bat_cap,d_s);

save(cs_cycle,'cs');

%% Emissions
S4_Emissions_calculation(preq);
```

The first script simply collects the various information concerning ICE type, Gearbox and Electric Machines, calculates inertia due to them and gives in output a more compact workspace.

```
function
pwt=S1_Powertrain_generator(en_type,gbx_type,fm_type,rm_type,bat_type)
en=load(en_type);
gbx=load(gbx_type);
fm=load(fm_type);
rm=load(rm_type);
bat=load(bat_type);

J_pwt_f=en.J_eng+fm.J_em*(fm.em_to_en)^2;
J_pwt_r=rm.J_em*(rm.em_to_en)^2;

pwt=sprintf('%s %s %s %s %s',en_type, fm_type, rm_type, gbx_type, bat_type);
save(pwt);
```

```
end
```

The second script instead calculates the Cycle Power requirement independently from the cycle provided: it is essential to give only the cycle trace and, if required, the gear selection strategy (but it will be discussed later in another script). It is not even necessary due to the fact that the powertrain subject of study is an automatic, and practically all the hybrid powertrains are due to optimization of fuel consumption.

Each point of the cycle trace is considered and it is calculated the power needed for motion for each gear of the forward axle plus the one for the rear axle with the gearbox clutch open (inertias are accounted in both cases, the second one it is obviously lower due to the absence of gearbox and ICE inertias), it is explained the reasons of this approach in the next script. Knowing the speed in each point even the ICE and Rear EM speed is calculated and thus the torque for each gear and each point is calculated.

Furthermore, a cycle power requirement is calculated as prescribed in the WLTP, in order to verify the break-off condition. It is possible to vary the coast down coefficients if needed or to calculate them following the prescription given by the WLTP procedure.

```
%%% Cycle Power requirement calculation
function preq=S2_Cycle_P_req(veh,cy,pwt)
load(veh);

ndv_i=(tau*tau_f*60)/(2*pi*R*3.6);                              %   [rpm*h/km]
Ratio of engine speed and velocity for each gear
ndv_i(end+1:end+(size(rm.em_to_en,2)))=rm.em_to_en*(60)/(2*pi*R*3.6);
i_max=length(tau);    %   []          Number of maximum forward gears
TM=m_u+100+0.15*(m_l-m_u-100);   %   [kg]     WLTP Test Mass of the vehicle
F0=TM*0.140; F1=0; F2=2.8*10^-6*TM+0.017*w*h; %   []Coefficients from
calculation methods

load(cy);
%% Calculations of required power

a(1:length(v),:)=0;
a(1:length(v)-1,:)=(v(2:length(v))-v(1:length(v)-1))/3.6;     %   [m/s^2]
Vehicle acceleration at second
m_tras=(TM+J_w/(R^2)+(tau).^2*J_pwt_f*tau_f^2/(R^2)+J_pwt_r(1)/(R^2));
m_tras(end+1:end+(size(rm.em_to_en,2)))=(TM+J_w/(R^2)+J_pwt_r./(R^2));
P_req=((F0*v+F1*v.^2+F2*v.^3)+a.*v*m_tras)./(3600*eta_f);             %
[kW]        Power required to overcome driving resistance and to accelerate
P_req(:,1:length(eta))=P_req(:,1:length(eta))./eta(1:length(eta));

n_i=v*ndv_i;

T_req=P_req./n_i*1000*60/(2*pi);
```

```
T_req(isnan(T_req))=0;

F(2:length(v),:)=F0+F1*(v(2:length(v))+v(1:length(v)-
1))/2+F2*((v(2:length(v))+v(1:length(v)-1))/2).^2+a(2:length(v))*TM*1.03;
d(2:length(v),:)=(v(2:length(v))+v(1:length(v)-1))/2/3.6.*(t(2:length(v))-
t(1:length(v)-1));

E=(F.*d);
E(F<0)=0;
E_tot=cumtrapz(E);
E_cycle=E_tot(end);

cycle=table(t,v,P_req,T_req,n_i);

preq=sprintf('%s %s %s',cy,veh,pwt);
save(preq,'cycle','E_cycle');
```

The third script simulates the behaviour of the Hybrid ECU of the car. A Hybrid ECU must decide, instant by instant, if the required power and torque must be split between the EMs and the ICE according to various signals. Being this a simplified model, it is considered only the ICE/P4 configuration (although the P1f is easily implementable), with regenerative braking.

The script checks the state of charge of the battery, if above a selected threshold check upon the maximum power, torque and speed exploitable by the P4 machine. If below these thresholds for the specific point proceed with the calculation of the instantaneous power demanded from the P4 EM and subtracts the energy for the battery. If any of the above fails it switches to the ICE but checking each gear and selecting the most efficient one (the one with the lowest fuel consumption) and then adding the grams of consumed fuel. In the main script after the call of this subroutine is checked whether the breakoff condition is fulfilled or not.

```
%%% Powertrain logic
function hy=S3_powertrain_logic(pwt,cycle,bat_cap,d_s)
load(preq);
load(pwt,'en','fm','rm','bat');

bat_en(1,1)=bat_cap;
exp_el_P(height(cycle),:)=0;
en_on=exp_el_P; gear=en_on; fc=en_on;
k=1;
r_g=size(rm.em_to_en,2);
i_max=size(cycle.P_req,2)-r_g;

for i=2:height(cycle)
    for l=1:r_g
        if cycle.P_req(i,i_max+l)>0
            if (bat_en(i-1,k)>bat.max_cap*bat.min_cap_p) % Battery is above
minimum SOC
                el_P(1:i_max+l)=NaN(1);
                j=i_max+l;
```

```
                if (cycle.n_i(i,j)<max(rm.e_curve.n)) % Electric motor
maximum speed is above road speed
el_eff(j)=max(rm.e_eff.eff(cycle.P_req(i,j)>rm.e_eff.P));
if(cycle.P_req(i,j)<cycle.n_i(i,j)*interp1(rm.e_curve.n,rm.e_curve.T,cycle.n_
i(i,j),'spline')/60*2*pi/10^3) % Electric motor maximum power at given speed
is above requested speed
                        el_P(j)=cycle.P_req(i,j)/el_eff(j);
                        en_on(i,:)=0;
                    else
                        en_on(i,:)=3;
                    end
                else
                    en_on(i,:)=2;
                end
                exp_el_P(i,k)=el_P(j);
            else
                en_on(i,:)=1;
            end
        end
        if cycle.P_req(i,i_max+1)<0
            if (bat_en(i-1,k)<bat.max_cap)
                j=i_max+1;
                if (cycle.n_i(i,j)<max(rm.e_curve.n))
                    el_eff(j)=max(rm.e_eff.eff((-
cycle.P_req(i,j))>rm.e_eff.P));
                    if(-cycle.P_req(i,j)<cycle.n_i(i,j)*
interp1(rm.e_curve.n,rm.e_curve.T,cycle.n_i(i,j),'spline')/60*2*pi/10^3)
                        el_P(j)=cycle.P_req(i,j)*el_eff(j)*bat.reg_eff;
                    else
                        el_P(j)=NaN(1);
                    end
                else
                    el_P(j)=NaN(1);
                end
                exp_el_P(i,k)=el_P(j);
            end
        end
    end
    if en_on(i,:)>0
        for j=1:size(cycle.P_req,2)-1
            if (cycle.n_i(i,j)<max(en.full_load.n)&&(cycle.P_req(i,j)>0))
                if (j==1&(cycle.n_i(i,j)<min(en.full_load.n)))

en_c(j)=interp2(en.n,en.bmep,en.FC,min(en.full_load.n),cycle.T_req(i,j)/(en.V
*10^2)*(2*pi*2),'spline');
                else
if(cycle.P_req(i,j)<cycle.n_i(i,j)*interp1(en.full_load.n,en.full_load.bmep*e
n.V/(2*pi*2)*10^2,cycle.n_i(i,j),'spline')/60*2*pi/10^3)
en_c(j)=interp2(en.n,en.bmep,en.FC,cycle.n_i(i,j),cycle.T_req(i,j)/(en.V*10^2
)*(2*pi*2),'spline');
                    else
                        en_on(i,:)=4;
new_n=interp1(en.full_load.n.*en.full_load.bmep*en.V/(2*pi*2)/10^2,en.full_lo
ad.n,cycle.P_req(i,j),'spline');
en_c(j)=interp2(en.n,en.bmep,en.FC,new_n,cycle.P_req(i,j)*60*2/(new_n*en.V*10
^2),'spline');
                    end
                end
            else
                en_on(i,:)=5;
                en_c(j)=0;
```

```
            end
        end
        [fc(i,k),gear(i,k)]=min(en_c);
    end
    if isnan(exp_el_P(i,k))
        exp_el_P(i,k)=0;
    end
    bat_en(i,k)=bat_en(i-1,k)-exp_el_P(i)/3600;
end
d=d_s+cumtrapz(cycle.t,cycle.v/3.6)/1000;
hy=table(bat_en,exp_el_P,en_on,fc,gear,d);
end
```

The last subroutine simply analyses the CD and CS cycles to extract the CO2 emissions and from them calculate the combination of the two considering the UF. At the moment the UF curve is the one of the EU legislation, but as everything in this model, could be easily varied to accommodate a different legislation (Japanese or US) or totally different test cycles.

The consumption is derived from the CO2 emissions as prescribed by the WLTP standard, even if, due to the simulation the CO2 emissions are directly calculated from the instantaneous fuel consumption.

```
%%% Emissions calculation
function S4_Emissions_calculation(cd_cycle,cs_cycle)
load(cd_cycle);
load(cs_cycle);
C=[26.25; -38.94; -631.05; 5964.83; -25094.60; 60380.21; -87517.16; 75513.77;
-35748.77; 7154.94];
d_n=800;
cycle_del=[1 600 1026 1478 1801];

for i=1:(length(brake_off_c)-1)
    commandLine = sprintf('hy=cycle%d;', i);
    eval(commandLine);
    for j=1:(length(cycle_del)-1)
        cons((i-1)*4+j,:)=sum(hy.fc(cycle_del(j):cycle_del(j+1)))/835;
        d((i-1)*4+j,:)=hy.d(cycle_del(j+1));
        mCO2((i-1)*4+j,:)=
sum(hy.fc(cycle_del(j):cycle_del(j+1)))/(0.0315*10^3);
        cons100_km((i-1)*4+j,:)=cons((i-1)*4+j,:)/(hy.d(cycle_del(j+1))-
hy.d(cycle_del(j)))*100;
        mCO2_km((i-1)*4+j,:)=cons100_km((i-1)*4+j,:)*0.835/0.0315;
    end
    ph_type((i-1)*4+1:(i)*4,1)=["L","M","H","EH"];
end
UF=0;
for i=1:size(d,1)
    exp_C_c=0;
    for j=1:length(C)
        exp_C_c(j)=(-C(j)*(d(i)/d_n)^j);
    end
    exp_C=sum(exp_C_c);
    UF(i,:)=1-exp(exp_C)-sum(UF);
end
CD=table(cons100_km,mCO2_km,d,UF,ph_type);
```

```
mCO2_CD=sum(CD.UF.*CD.mCO2_km)/sum(CD.UF);

clear ('cons100_km','mCO2_km','d','UF','ph_type','cons','mCO2');
hy=cs; i=1;
ph_type((i-1)*4+1:(i)*4,1)=["L","M","H","EH"];
for j=1:(length(cycle_del)-1)
        cons((i-1)*4+j,:)=sum(hy.fc(cycle_del(j):cycle_del(j+1)))/835;
        d((i-1)*4+j,:)=hy.d(cycle_del(j+1));
        mCO2((i-
1)*4+j,:)=sum(hy.fc(cycle_del(j):cycle_del(j+1)))/(0.0315*10^3)*100;
        cons100_km((i-1)*4+j,:)=cons((i-1)*4+j,:)/(hy.d(cycle_del(j+1))-
hy.d(cycle_del(j)))*100;
        mCO2_km((i-1)*4+j,:)=cons100_km((i-1)*4+j,:)*0.835/0.0315;
end
CS=table(cons,mCO2,d,ph_type);
mCO2_CS=sum(CS.mCO2)/CS.d(end);
mCO2_tot=sum(CD.UF.*CD.mCO2_km)/sum(CD.UF)+mCO2_CS*(1-sum(CD.UF));

save("emissions",'CD','CS','mCO2_CD','mCO2_CS','mCO2_tot');
end
```

3.4. Simulation of 3 4WD P4 C-Segment vehicles

For the purpose of simulation there was selected a reference vehicle of the group in the C-segment (J/M variant) in its original 4WD gasoline powered form and in a hybridized form. 2 competing vehicles from different carmakers were also considered taking data publicly available.

Vehicle 1, taken as a reference uses an AT6 transmission and a fictious ICE engine map. The engine is a turbocharged gasoline one. Weights and dimensions are the original one declared from the carmaker.

Its hybridized form uses the same ICE and gearbox with the addition of a P4 EM.

Vehicle 2 has a turbocharged gasoline engine with an AT6 transmission. The gear ratios were the one publicly available as the full load map. The fuel consumption map instead is the same of the reference ICE engine.

Vehicle 3 has a naturally aspirated engine with a fixed drive (it corresponds to a 5^{th} gear in the other 2 vehicles more or less). The fuel consumption of this vehicle is 20% higher than the other two. The full load map has been scaled manually according to the one declared by the carmaker.

The various test masses were calculated according to the prescribed normative.

In table 5 and 6 some data normalized with respect to Vehicle 1. The relative energy is a function of the theoretical mechanical energy expended during the WLTP cycle by Vehicle 1.

	Vehicle 1	Vehicle 1 Hybridized	Vehicle 2	Vehicle 3
Curb mass	100%	123%	118%	125%
Laden mass	100%	100%	82%	125%
Rolling Radius	100%	100%	95%	102%
Height	100%	100%	92%	101%
Width	100%	100%	100%	100%
Curb/Laden mass ratio	182%	148%	126%	181%
Relative energy stored in HV battery		181%	121%	190%
Test mass	100%	117%	109%	124%
F0	100%	117%	109%	124%
F2	100%	101%	93%	103%
Test/Curb mass ratio	118%	112%	109%	117%

Table 5 – Size characteristics of 3 different 4WD P4 hybrid vehicles

	Vehicle 1	Vehicle 1 Hybridized	Vehicle 2	Vehicle 3
ICE relative power	100%	100%	70%	63%
P4 (Relative to ICE Vehicle 1)		85%	46%	42%
Total hybrid relative power	100%	185%	116%	105%
Maximum velocity		104%	103%	87%
Maximum velocity in electric mode		104%	64%	61%

Table 6 - Power and speed characteristics of 3 different 4WD P4 hybrid vehicles

The results regarding the WLTP CO2 emissions were in line with the declared NEDC emissions from the manufacturers, being the Vehicle 3 the winner of the lot, while Vehicle 1 Hybridized was shortly followed by Vehicle 2, despite being heavier. All the emissions are normalized with respect to the one emitted by Vehicle 1 during a WLTC run.

	Vehicle 1	Vehicle 1 Hybridized	Vehicle 2	Vehicle 3
Relative CO2 g/km combined	1	25%	32%	18%
WLTC in charge depleting		4	4	5
Relative CO2 g/km CS mode		89%	74%	56%

Table 7 - WLTP emission result of 3 different 4WD P4 hybrid vehicles

It has to be noted that neither Vehicle 2 nor Vehicle 3 are capable of completing a WLTC cycle without switching on the ICE due to limitation in speed in the P4 electric machine. Since the Vehicle 1 Hybridized is capable of completing a WLTC cycle without switching on the ICE, a further investigation was developed.

Each of the vehicle had a battery pack limited net energy capacity to 75% of the gross energy capacity declared by the manufacturer (as declared by one of them). Since Vehicle 1 Hybridized almost completed even the second WLTC run without switching on the ICE the battery model was slightly modified moving the ratio between the net and the gross energy capacity from 75% to 80%.

The Vehicle was not only able to complete the second WLTC run without switching on the engine, but also had a significant reduction of emissions in the Charge Sustain mode.

	Vehicle 1	Vehicle 1 Hybridized	Vehicle 3	Vehicle 1 Hybridized 2
Relative energy stored in HV battery		181%	190%	193%
Relative CO2 g/km combined	1	25%	18%	1%
WLTC in charge depleting		4	5	5
Relative CO2 g/km CS mode		89%	56%	3%

Table 8 - WLTP run with enhanced battery capacity

These results may be not quantitatively significant due to many flaws of the model, first of all the "ECU" sub model that is too discrete with his thresholds and does not reflect at all a production Hybrid ECU, being simplified. But these result underlines that a vehicle capable of completing at least two WLTC runs without turning on the ICE could really improve its emissions and that the size of the battery is significant also in the Charge Sustain mode, especially if the test procedure chosen is a chain of the Charge Depleting cycle and the Charge Sustain one.

Due to the saturation of the UF factor curve (figure 50) is evident that a further improvement in numbers of consecutive WLTC runs (after 45 km the value is above 0.7) at the expense of added weight in the battery pack would not justify the variation, with the risk of being counterproductive. Instead concentrating the researches toward an improvement of the Charge Sustain cycle is much more convenient.

3.5. Conclusions and further improvements of the model

One of the principal limitation of this model is due to the data available. No efficiency model is present in the Electrical part of the Hybrid system, nor for the P4 engine neither for the HV Battery Pack. The coast down coefficients, being calculated from the WLTP standard are strongly pessimistic when compared to real ones (almost the double of measured ones) but calculating through the WLTP procedure is the only method to obtain these uniformly without having direct access to the vehicles and a test bed.

It is advisable also to integrate the P1f with an appropriate control strategy and investigating the advantages of using the ICE both powering the wheels and charging the battery in certain situations, due to improved efficiency of the ICE combustion that could be exploited to recharge the batteries and avoid the switching on of the ICE during successive conditions, taking into account that it couldn't be used as a cycle beating strategy but as a general optimization of the energy consumed by the powertrain. Further investigation upon thresholds for enabling the regeneration mode of the ICE is important.

Another important improvement to be done on the model is the correction method of the emission calculation especially regarding the energy balance for the CS cycle.

The last consideration is that this is a steady-state cycle with absolutely no errors and variability, so two Simulink model simulating the test conditions and the Hybrid ECU are vital to be integrated in a further evolution of the model.

Bibliography

E/ECE/324/Rev.2/Add.100/Rev.3−E/ECE/TRANS/505/Rev.2/Add.100/Rev.3. (s.d.).

Environmental Policy Division, Road Transport Bureau, Ministry of Land, Infrastructure, Transport and Tourism, Japan. (s.d.). *Development of the Japan's RDE (Real Driving Emission) procedure.*

Jelica Pavlovic, A. T. (s.d.). The Impact of WLTP on the Official Fuel Consumption and Electric Range of Plug-in Hybrid Electric Vehicles in Europe.

L 175/2017 EU Regulation. (s.d.).

Official Journal of the European Union L 375 of 27 December 2006 . (s.d.).

Sims R., R. S.-N. (s.d.). Climate Change 2014: Mitigation of Climate Change. Contribution of Working Group III to the Fifth Assessment Report of the Intergovernmental Panel on Climate Change.

Thomas R. Andersona, E. H. (n.d.). CO2, the greenhouse effect and global warming: from the pioneering work of Arrhenius and Callendar to today's Earth System Models. *Endeavour Vol. 40 No.3*.